

FUNDAMENTAL ASPECTS OF SURFACTANT-POLYMER FLOODING PROCESS

D. O. SHAH

*Department of Chemical Engineering and Anesthesiology,
University of Florida, Gainesville, Florida 32611*

ABSTRACT

Surfactant-polymer flooding process offers a promising approach to recover additional oil from the water flooded reservoirs which may contain as much as 70% of original oil-in-place. The capillary number, which determines the microscopic displacement efficiency of oil, can be increased by 3 to 4 orders of magnitude by reducing the interfacial tension (IFT) of oil ganglia below 10^{-3} dynes/cm. Conceptual events involved in the mobilization and displacement of oil ganglia are described including the role of ultralow interfacial tension, the role of interfacial viscosity in coalescence of oil ganglia and formation of the oil bank, the propagation of the oil bank, the surfactant-polymer incompatibility, the formation and flow of emulsions in porous media, the role of wettability as well as the influence of surface charge density of the rock/fluid interface and oil-brine interface in oil displacement efficiency. It is shown that there are two regions of ultra-low IFT; 1) in the low surfactant concentration (0.1-0.2%) and the other in the high surfactant concentration region (2.0%-10.0%). In the low concentration systems, the ultra-low interfacial tension occurs when the aqueous phase of the surfactant solution is about the apparent critical micelle concentration. And, the salinity is at the critical electrolyte concentration for the coacervation process. The migration of surfactant from the aqueous phase to the oil phase via coacervation process appears to be responsible for the ultralow interfacial tension.

In high surfactant concentration systems, a middle phase microemulsion in equilibrium with excess oil and brine forms in a narrow salinity range. The salinity at which equal volumes of oil and brine are solubilized in the middle phase microemulsion is referred to as the optimal salinity of the system. At the optimal salinity, the interfacial tension at both interfaces is equal. Evidence is presented that the middle phase microemulsion at the optimal salinity is a water external microemulsion formed due to coacervation and subsequent phase separation of micelles from the aqueous phase. The optimal salinity can be shifted to a desired value by varying the structure and concentration of alcohol. The shift in optimal salinity can be correlated with the brine solubility of the alcohol used in a given surfactant formulation. It was further observed that the optimal salinity increases with the oil chain length. In order to form middle phase microemulsions at very high salinity, ethoxylated surfactants or alcohols can be incorporated into a surfactant formulation which can shift the optimal salinity to as high as 32% NaCl concentration. Such high salinity formulations consisting of petroleum sulfonates and ethoxylated sulfonates are relatively insensitive to divalent cations.

The coalescence rate or the phase separation time was minimum at optimal salinity. It was also observed that the apparent viscosity was minimal at the optimal salinity for the flow of microemulsions through porous media. The rate of flattening of an oil drop in a surfactant formulation increases strikingly in the presence of alcohol. It appears that the presence of alcohol promotes the mass transfer of surfactant from the aqueous phase to the interface. The addition of alcohol also promotes the coalescence of oil drops, presumably due to a decrease in the interfacial viscosity.

The surfactant-polymer incompatibility can lead to a phase separation of a surfactant and polymer even in the absence of oil. In the presence of oil, the formation of middle phase microemulsion is promoted by the presence of polymer in the aqueous phase. The surfactant-polymer incompatibility is explained in terms of excluded volume effects and the maximization of solvent for polymer molecules.

Some novel concepts for surfactant-polymer flooding process have been discussed including the use of two different surfactant slugs, two different polymer slugs, salinity gradient design and the injection of an oil bank to promote oil recovery.

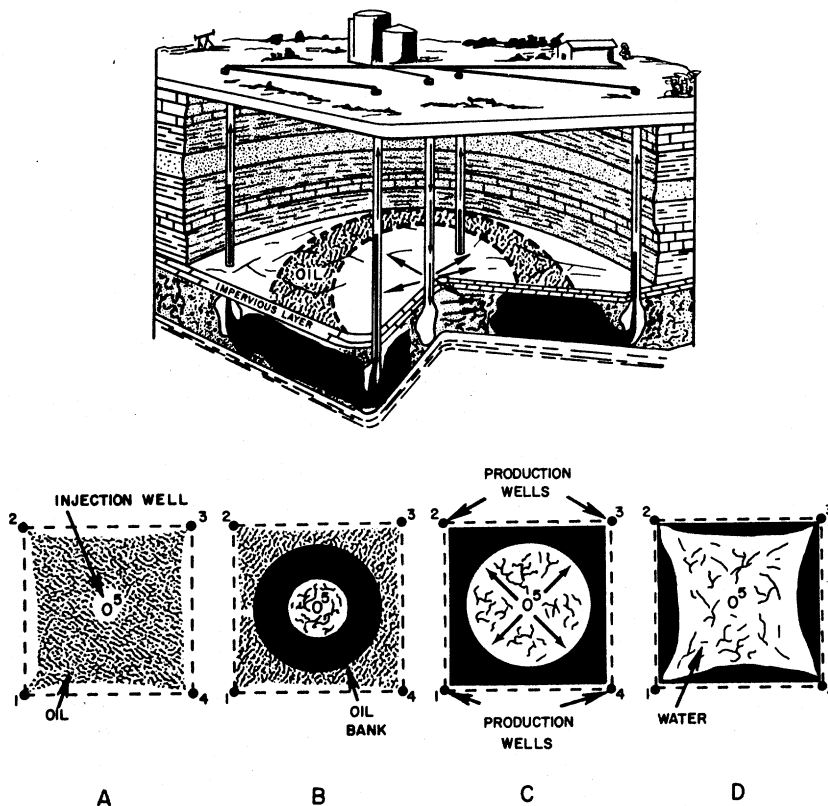


Fig. 1 Schematic diagram of an oil reservoir and the displacement of oil by water or chemical flooding.

A. INTRODUCTION

It is well recognized that the energy consumption per capita and the standard of living of a society are interrelated. Among various sources of energy, fossil fuels or crude oils play an important role in providing the energy supply of the world. It also serves as a raw material for feed stocks in chemical industry. In view of the worldwide energy crisis, the importance of enhanced oil recovery to increase the supply of crude oil is obvious and various enhanced oil recovery processes have been proposed and tested both on a laboratory scale and in the field. For heavy oils, thermal processes have been used extensively whereas for light oils, chemical processes such as polymer flooding, caustic flooding, miscible flooding and surfactant-polymer flooding have attracted great interest. The major research findings in the enhanced oil recovery area have been reported in recent literature and the symposia proceedings of various conferences during the last decade (1-11). The present paper focuses on the fundamental aspects of the surfactant-polymer flooding process and related phenomena.

Figure 1 schematically shows a three-dimensional view of a petroleum reservoir.

At the end of water-flooding, the oil that remains in the reservoir is believed to be in the form of oil ganglia trapped in the pore structure of the rock as shown in Figure 1A. These oil ganglia are entrapped due to capillary forces. However, if a surfactant solution is injected to lower the interfacial tension of the oil ganglia from its value of 20-30 dynes/cm to 10^{-3} dynes/cm, the oil ganglia can be mobilized and can move through narrow necks of the pores. Such mobilized oil ganglia form an oil bank as shown in Figure 1B. Figures 1C and 1D schematically show the oil bank approaching the production well and the subsequent breakthrough of the drive water. Figure 2 schematically illustrates a two-dimensional view of the surfactant-polymer flooding process.

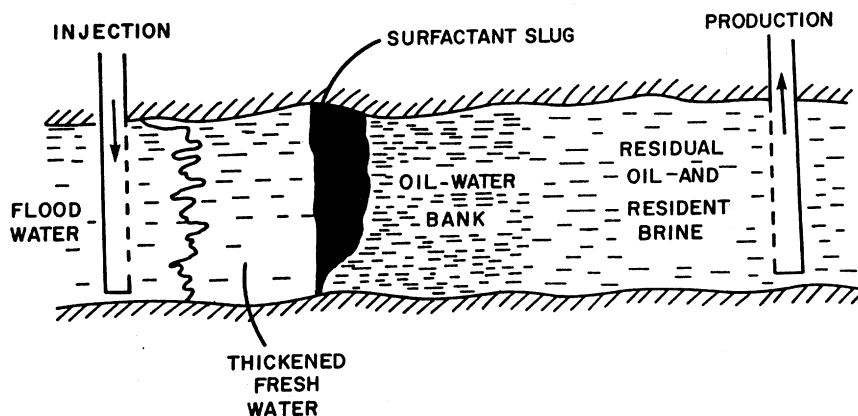


Fig. 2 Schematic diagram of the surfactant-polymer flooding process.

The surfactant slug is followed by a polymer slug for a proper mobility control of the process.

B. CAPILLARY NUMBER AND CONCEPTUAL ASPECTS OF THE PROCESS

Recently, in an excellent review article, Taber (12) has summarized various empirical dimensionless numbers proposed by several investigators to correlate the oil displacement efficiency in porous media. Figure 3 shows such a correlation reported by Foster (13) between the capillary number and residual oil in porous media.

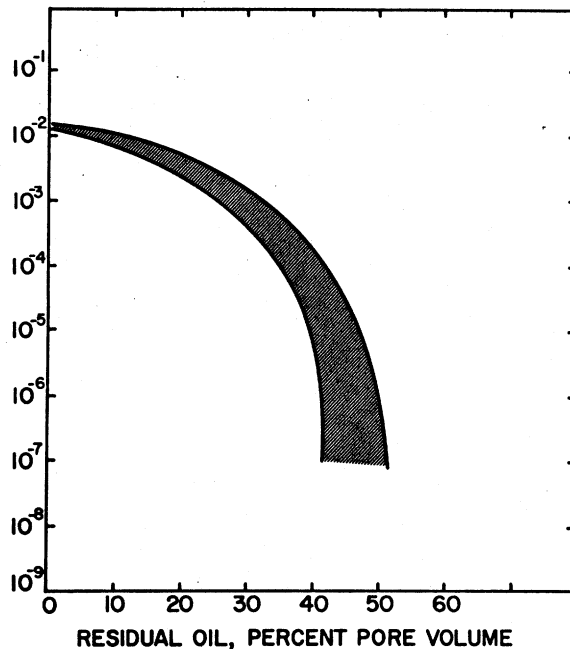


Fig. 3 Dependence of residual oil saturation on Capillary Number (Foster, W.R., J. Pet. Tech., p. 206, Feb. 1973).

The capillary number represents the ratio of viscous to capillary forces (i.e. $N_{ca} = \mu v / \sigma \phi$ where μ and v are the viscosity and velocity of the displacing fluid, σ is the interfacial tension and ϕ is the pore volume). At the end of water flooding, the capillary number is around 10^{-6} and this number has to be increased by 3 to 4 orders of magnitude for tertiary oil recovery processes (14). Under practical reservoir conditions, the reduction in interfacial tension from a high value of 20 or 30 dynes/cm to 10^{-3} or 10^{-4} dynes/cm offers such a possibility. Therefore, the main function of the surfactant is to produce such an ultra-low interfacial tension at the oil ganglia/surfactant formulation interface. Figure 4 schematically shows the role of ultralow interfacial tension in promoting the mobilization of oil ganglia in porous media. Subsequently, the displaced oil ganglia must coalesce to form an oil bank. For this a very low interfacial viscosity is desirable (Figure 5). It is known that high interfacial viscosity results in the formation of stable emulsion (15).

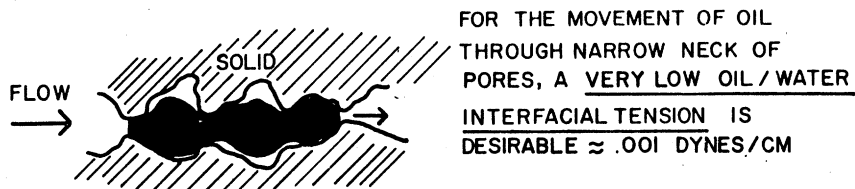


Fig. 4 Schematic diagram of the role of low interfacial tension in the surfactant-polymer flooding process.

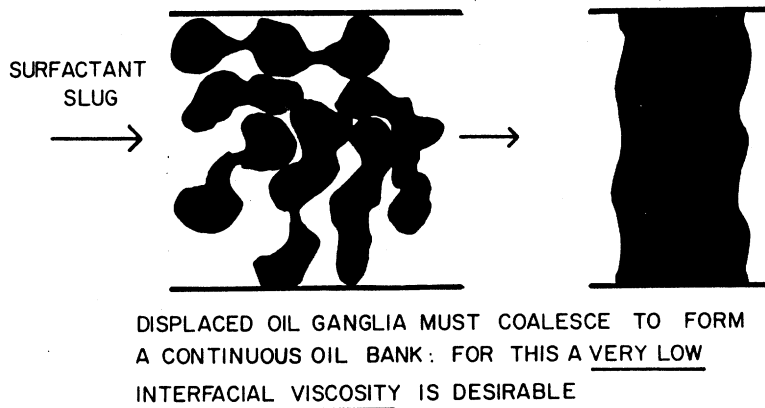


Fig. 5 Schematic diagram of the role of low interfacial viscosity in the surfactant-polymer flooding process.

Once an oil bank is formed in the porous medium, it has to be propagated through the porous medium without increasing the entrapment of oil at the trailing edge of the oil bank. As shown in Figure 6, the maintenance of ultralow interfacial tension at the oil bank/surfactant/slug interface is essential for minimizing the entrapment of the oil in the porous medium whereas the leading edge will coalesce with the oil ganglia.

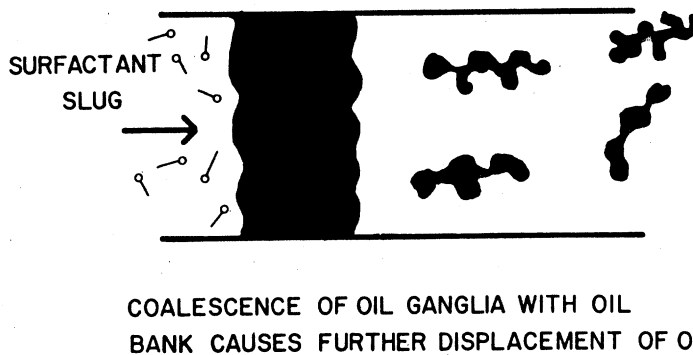


Fig. 6 Schematic diagram of the role of coalescence of oil ganglia in the surfactant-polymer flooding process.

Figure 7 schematically illustrates the movement of the oil bank, surfactant slug and the mobility control polymer slug in the porous medium.

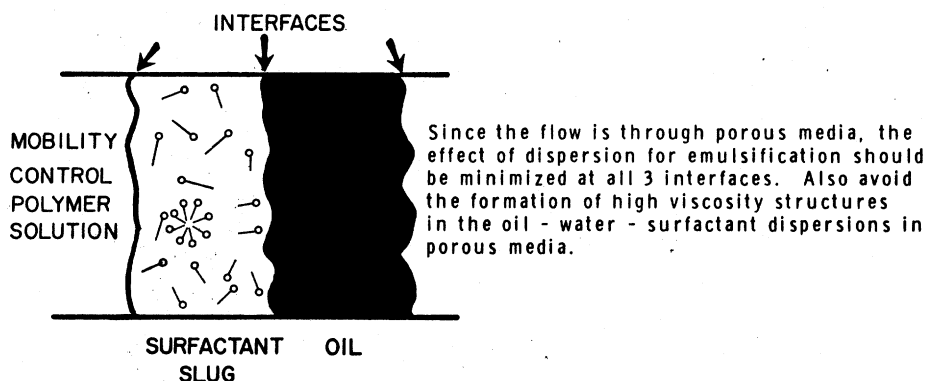
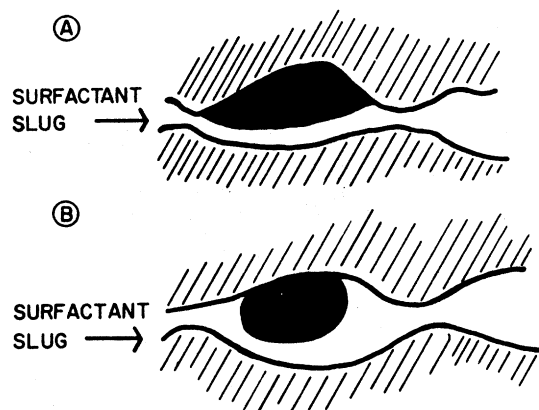


Fig. 7 Schematic illustration of the effects of dispersion and emulsification between the various slugs during the surfactant-polymer flooding process.

Since the flow through the porous medium causes dispersion of these fluids, emulsions will be formed at the oil bank/surfactant slug interface and a mixed surfactant-polymer zone will occur at the surfactant-polymer solution interface. High viscosity structures at both these interfaces should be avoided in order to improve the efficiency of the process. The mass transfer of surfactant to the oil bank can influence the magnitude of interfacial tension (16). Trushenski (17) has shown that surfactant-polymer incompatibility leading to a phase separation of surfactant and polymer strikingly reduces the efficiency of the process.



PROPER CHOICE OF SURFACTANT CAN CHANGE (A) TO (B)

Fig. 8 The role of wettability and contact angle on oil displacement.

Figure 8 schematically illustrates the role of wettability of solid surface on the oil ganglia.

The choice of surfactant can influence the wettability of the rock surface to oil and brine (12).

Another parameter that we have found (18, 19) that influences the interfacial tension and interfacial viscosity and oil recovery is the surface charge at the oil-brine as well as rock-brine interfaces. We found that a high surface charge density leads to a lower interfacial tension, lower interfacial viscosity and higher oil recovery (Figure 9).

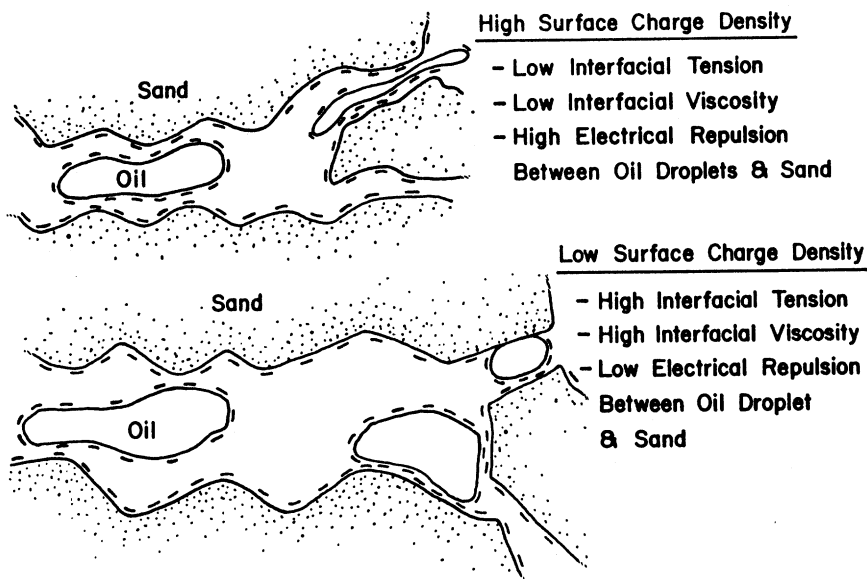


Fig. 9 Schematic diagram of the role of surface charge in the oil displacement process.

The conceptual processes described in Figures 3 to 9 are supported by the results of our studies described in the following sections.

C. LOW SURFACTANT CONCENTRATION SYSTEMS

Figure 10 shows the interfacial tension as a function of surfactant concentration in a dodecane/brine system.

It is evident that there are two regions of ultra-low interfacial tension (IFT). At low surfactant concentrations, the system appears to be a two-phase system, namely, oil and brine in equilibrium with each other, whereas at high surfactant concentration systems (around 4 to 8% surfactant concentration), a middle phase microemulsion exists in equilibrium with excess oil and brine. The formation of middle phase microemulsion and related phenomena will be discussed in section D.

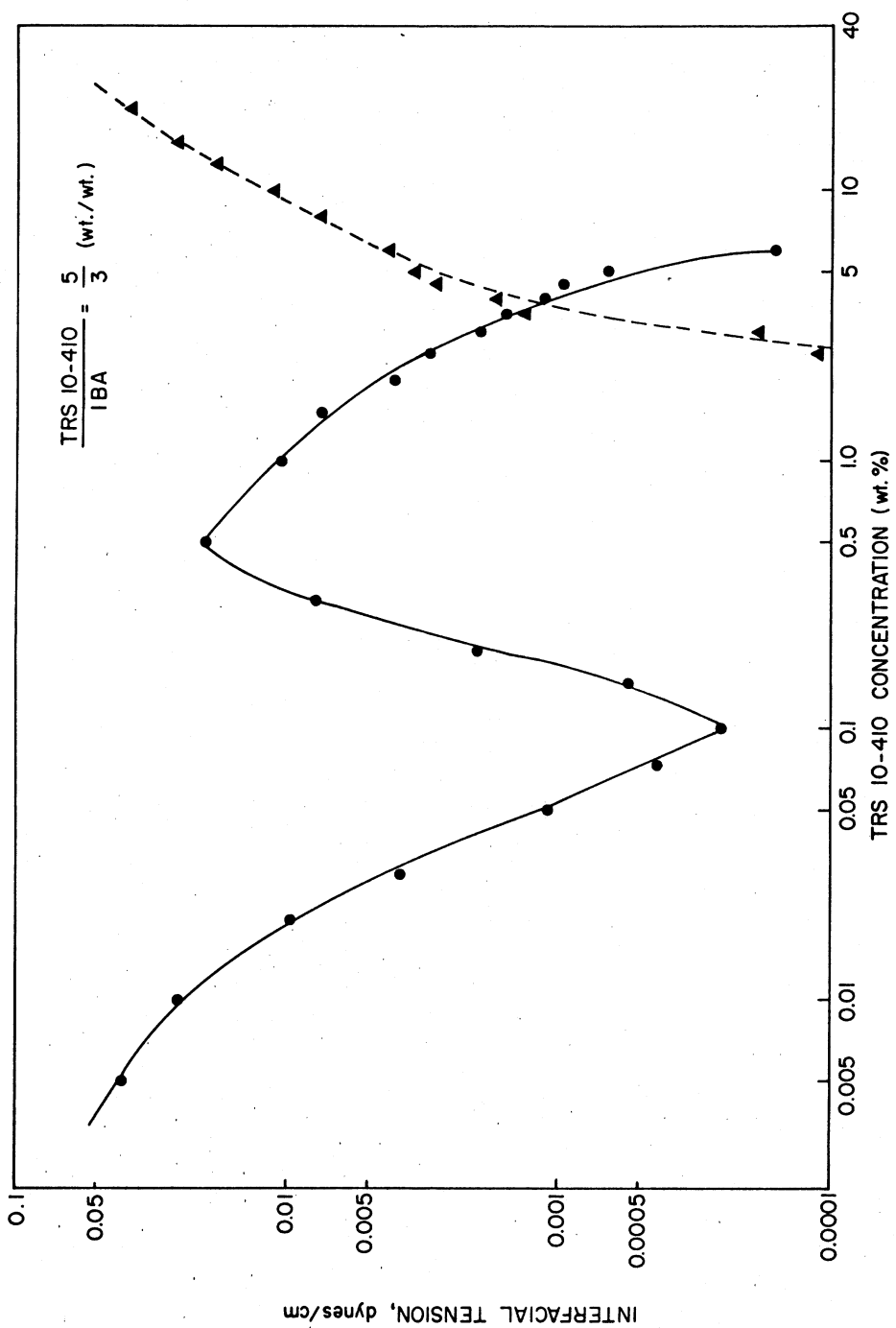


Fig. 10 Effect of surfactant concentration on the interfacial tension of TRS 10-410 + IBA in 1.5% NaCl with dodecane.

For low surfactant concentration systems, we have shown that the ultralow IFT occurs when surfactant molecules migrate from the aqueous phase to the oil phase (19-21). Figure 11 shows the interfacial tension and the partition coefficient of a surfactant in an octane/brine system. The ultra low IFT occurred around a partition coefficient of unity in this system (19,20). However, it should be emphasized that since the partition coefficient changes abruptly in this region the exact value of partition coefficient can vary significantly around ultralow IFT. We believe that a reasonable conclusion is that lowering of interfacial tension is observed when micelles leave the aqueous phase due to coacervation process (19-23).

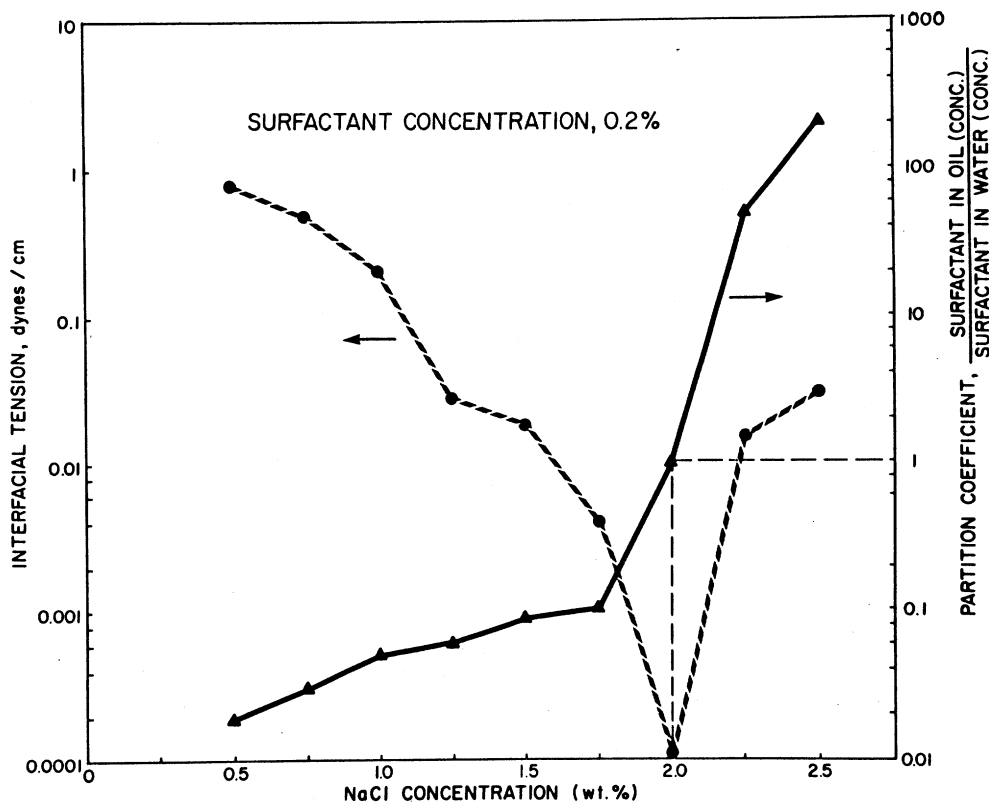


Fig. 11 Effect of added electrolyte on interfacial tension and surfactant partition coefficient of the system 0.2%TRS 10-80 + brine + octane.

Since commercial petroleum sulfonates involve a distribution of molecular weights and isomeric structures we also investigated the interfacial tension using isomerically pure sulfonates. Figure 12 shows the IFT behavior as a function of salinity, oil chain length and surfactant concentration using petroleum sulfonates (TRS 10-80 or TRS 10-410 and an isomerically pure surfactant UT-1). It is evident that both the salinity and oil chain length effects were similar for both these classes of sur-

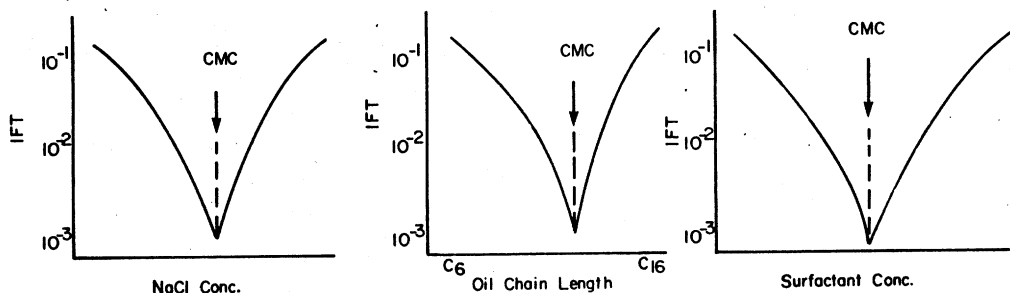
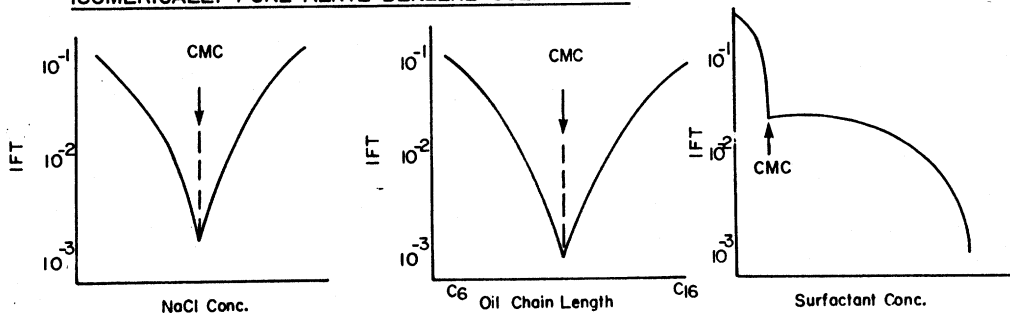
PETROLEUM SULFONATES:ISOMERICALLY PURE ALKYL BENZENE SULFONATES:

Fig. 12 Schematic diagram of the effect of salt concentration, oil chain length and surfactant concentration on the interfacial tension of pure and impure alkyl benzene sulfonates.

factants, namely, there is a specific salinity and specific oil chain length where we obtain an ultralow IFT. However, the effect of surfactant concentration on IFT was different for commercial and isomerically pure surfactants. For low surfactant concentration systems, we also observed that the ultra low IFT appears when the aqueous phase is at the apparent cmc for the surfactant remaining in the aqueous phase. These conclusions were in agreement with osmotic pressure, light scattering and spectroscopic measurements on the equilibrated aqueous phase (22).

Figure 13 is a generalized diagram showing the IFT, phase behavior and the two critical electrolyte concentrations for both pure and commercial surfactants at low as well as high surfactant concentrations. By direct analysis of surfactant concentrations in each phase, we found (21) that the salinity at which surfactant molecules leave the aqueous phase is lower than the salinity at which they enter the oil phase. Thus, we define two critical electrolyte concentrations, namely, CEC_1 , and CEC_2 , to represent the electrolyte concentrations at which the surfactant concentration begins to decrease in the aqueous phase and begin to increase in the oil phase respectively. We further observed that the minimum interfacial tension occurs in the vicinity of the first critical electrolyte concentration. In between CEC_1 and CEC_2 , the surfactant may precipitate or may form a coacervate phase below the aqueous phase or in between the aqueous and the oil phase depending upon its density (21).

In low concentration systems, it is possible that an extremely small volume of middle phase may exist between the oil and brine phases even though it may not be visible. This suggestion is in agreement with observation that the volume of the middle phase microemulsion increases linearly with the surfactant concentration and the straight line passes through the origin (24). It should be emphasized that the general behavior and inter-relationship shown in Figure 13 is valid for both commercial and isomerically pure surfactants (21).

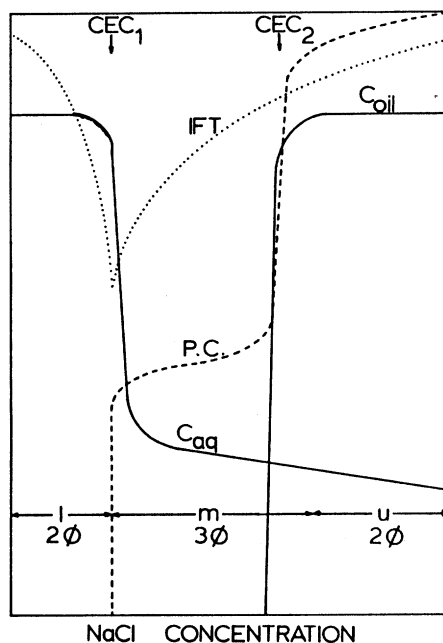


Fig. 13 Generalized diagram of the effect of salt concentration on surfactant partitioning, phase behavior and interfacial tension.

Figure 14 shows the effect of oil chain length on CEC_1 and CEC_2 in Aerosol OT/brine/oil systems. It is evident that the CEC_1 increases with oil chain length until it reaches the critical oil chain length (C_{11}) above which the value of CEC_1 remains constant. On the other hand, CEC_2 continues to increase with the oil chain length. Interestingly, we observed that the ultralow IFT only occurs for oil chain lengths below the critical oil chain length ($< C_{11}$), whereas the interfacial tension remains high for oils above the critical oil chain length (21).

We propose that all the oils below the critical oil chain length are able to solubilize in the micelles whereas the oils having chain length above the critical oil chain length are unable to solubilize in the micellar solution. Thus, it appears that solubilization of oil within the micelles is an important requirement for producing ultralow IFT. From our extensive studies on interfacial tension and partitioning of surfactant in relation to many parameters, we have proposed the following 5 necessary conditions to achieve ultralow IFT's.

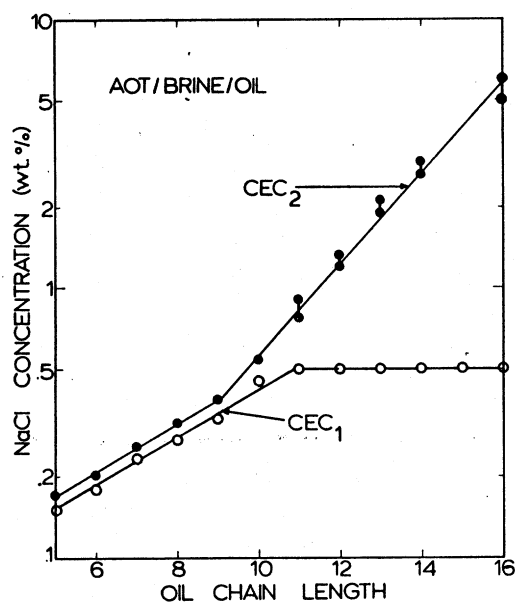


Fig. 14 Effect of oil chain length on the first and second critical electrolyte concentrations of Aerosol OT.

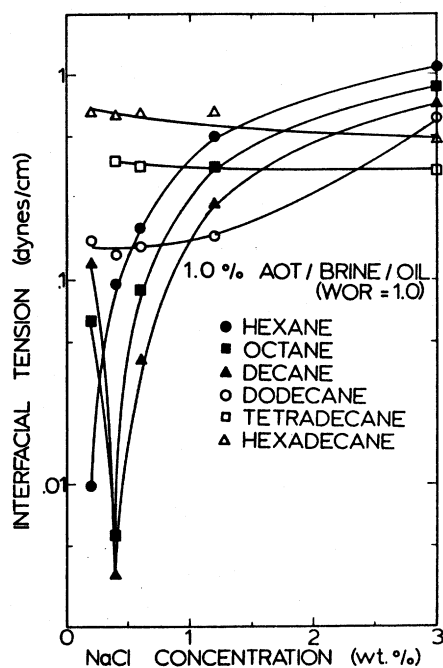


Fig. 15 Effect of oil chain length on the interfacial tension of the systems 1.0% AOT/brine/oil.

- 1) The total surfactant concentration should be appreciably above the apparent cmc in the aqueous phase.
- 2) The surfactant should be soluble in both the aqueous and the hydrocarbon phase.
- 3) Micelles in the aqueous phase should be able to solubilize oil from the hydrocarbon phase.
- 4) The aqueous phase salinity should be near the first critical electrolyte concentration (CEC_1).
- 5) There should be a large slope in the surfactant partition coefficient curve in the region of the ultralow IFT. (i.e. a steep partition coefficient curve for surfactant).

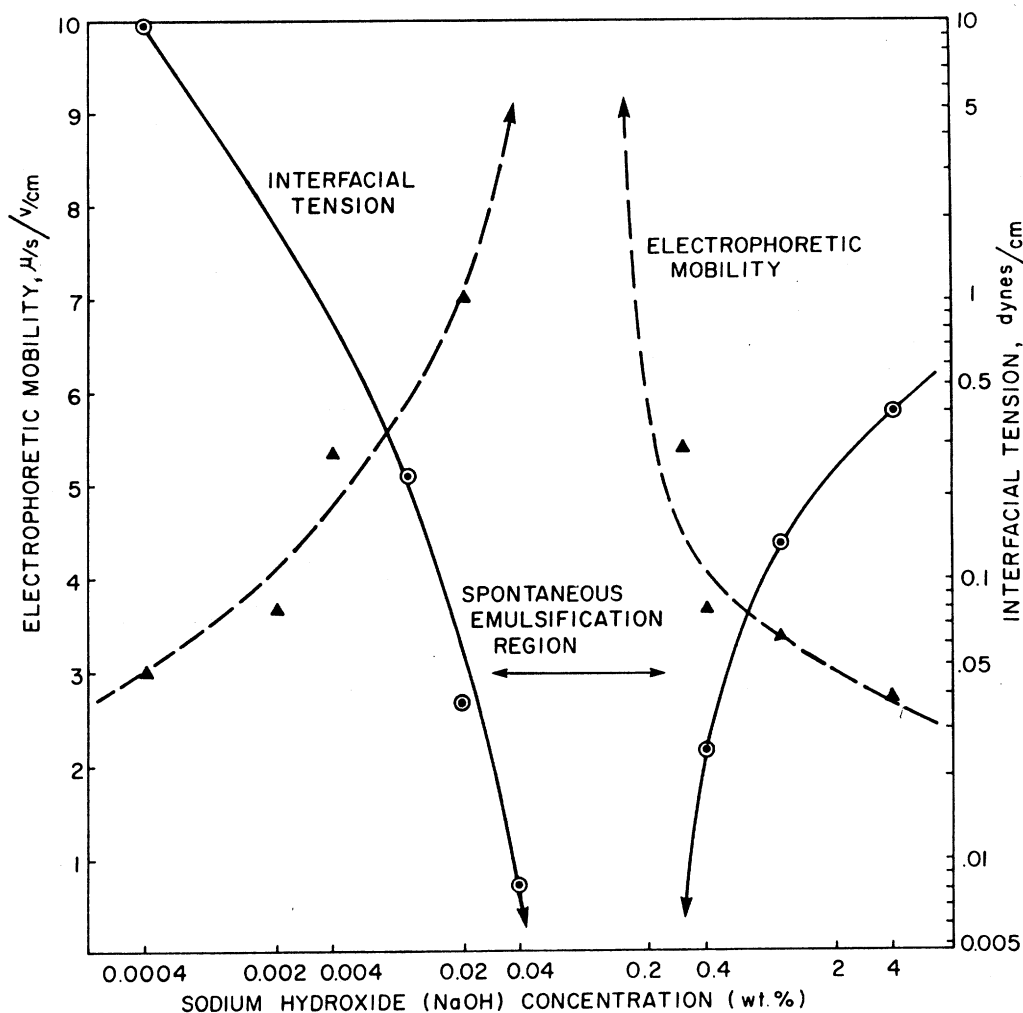


Fig. 16 A correlation between interfacial tension and electrophoretic mobility for crude oil-NaOH solutions.

Figure 16 shows the correlation of interfacial tension with electrophoretic mobility in crude oil/caustic systems (18,19,25,26). We have observed for several crude oils that the ultra low IFT occurs in the region where the electrophoretic mobility is maximum. This suggests that the maximum in surface charge density coincides with the minimum in interfacial tension. This correlation was also observed for the effect of salinity and surfactant concentration (19). Figure 17 schematically illustrates 3 components of the interfacial tension, namely, 1) surface concentration of the surfactant, 2) surface charge density, and 3) mutual solubilization of oil and brine. We propose that by adjusting any of these variables one can influence the magnitude of interfacial tension.

Using the conceptual approach shown in Figure 17, we were able to broaden and lower the magnitude of interfacial tension as well as increase the salt tolerance limit of the surfactant formulation.

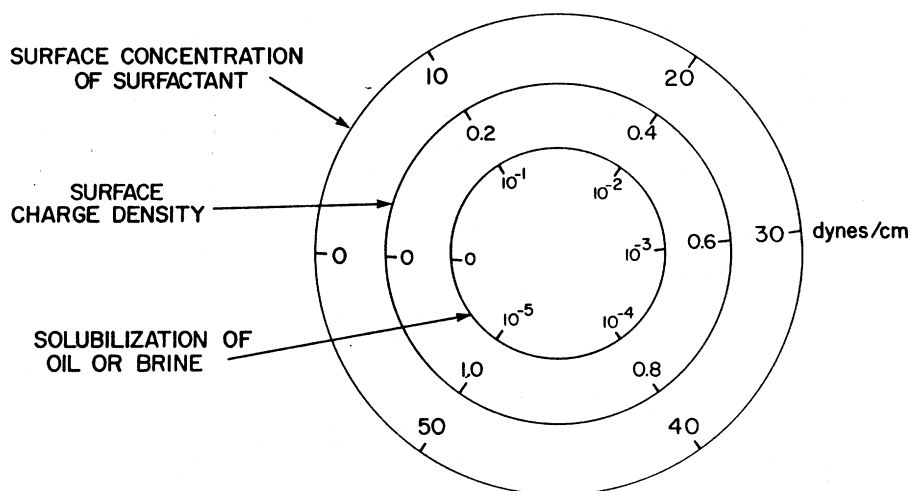


Fig. 17 A schematic illustration of the factors affecting the magnitude of the interfacial tension.

Figure 18 shows the interfacial tension of a petroleum sulfonate TRS 10-410/n-octane/brine system when gradually the petroleum sulfonate is replaced with an ethoxylated phosphate ester (Klearfac AA-270).

The Klearfac AA-270 containing a phosphate group possesses two ionic oxygen atoms and hence can generate a high surface charge density at the interface. This presumably is responsible for lowering the magnitude of IFT and broadening the salinity range over which the ultralow IFT occurs for the mixed surfactant systems (27).

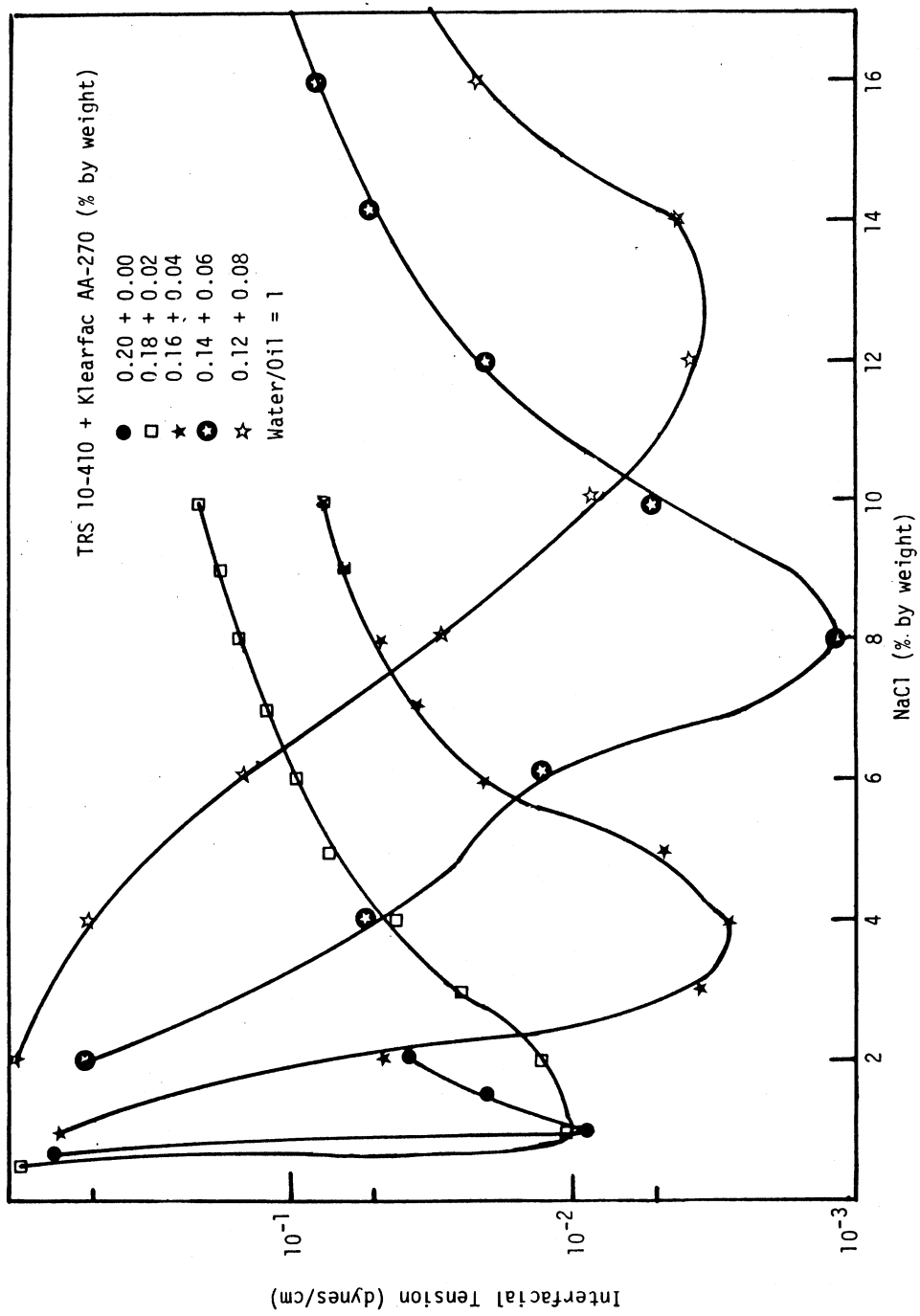


Fig. 18 An illustration of the reduction and broadening of the minimum in interfacial tension by the addition of Klearfac AA-270.

D. HIGH SURFACTANT CONCENTRATION SYSTEMS AND THE OPTIMAL SALINITY

Many surfactant formulations exhibit extreme flow or static birefringence in a given salinity range or in a given temperature range. Often these optically anisotropic formulations exhibit ultralow IFT with oil. The microstructure of such birefringent formulations should be of interest in understanding the changes in molecular associations occurring in these systems.

Figures 19-21 illustrate the microstructure of a birefringent surfactant formulation consisting of 5% TRS 10-410 + 3% isobutanol and 2% NaCl brine.



Fig. 19 Freeze-fracture electron micrograph of the anisotropic system 5% TRS 10-410 + 3% Isobutanol + 2% NaCl (8550 \times).

The freeze-fracture electron microscopic technique used to obtain these pictures is believed to preserve the microstructure of the samples due to the very rapid cooling rate (24). These electron micrographs clearly indicate that the birefringent formulations consist of bubbles filled with brine and separated from each other by a thin surfactant membrane. Figure 21 clearly shows the structure of this membrane consisting of several thin layers. The dimension of each layer is close to a surfactant bilayer (approximately 70Å). Therefore, it appears that when the salinity is increased in the surfactant formulation, the surfactant molecules form the multilayer structure while keeping their polar groups in contact with brine and form such cells or foamlike stable structure. We have called these structures birefringent cellular fluids (24).

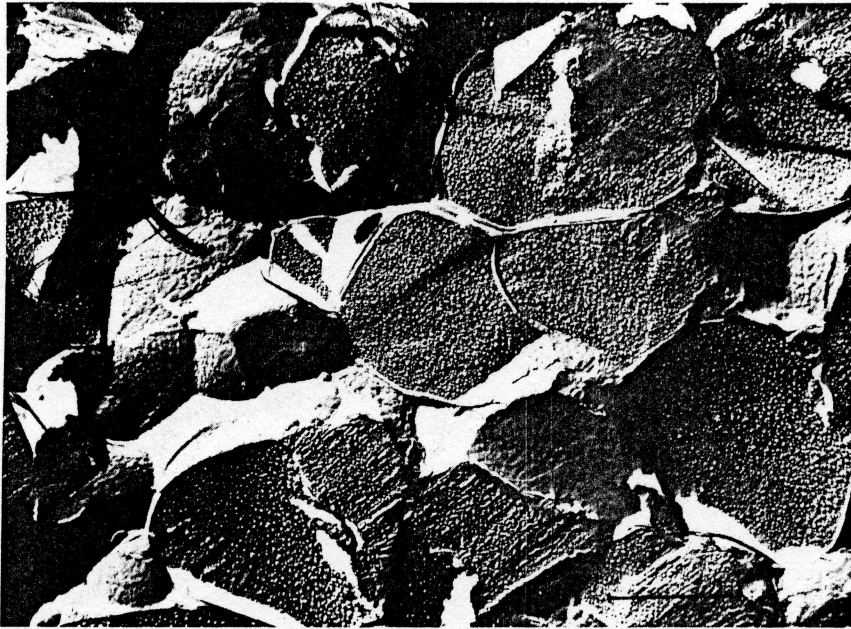


Fig. 20 Freeze-fracture electron micrograph of the above system at 18,000X.

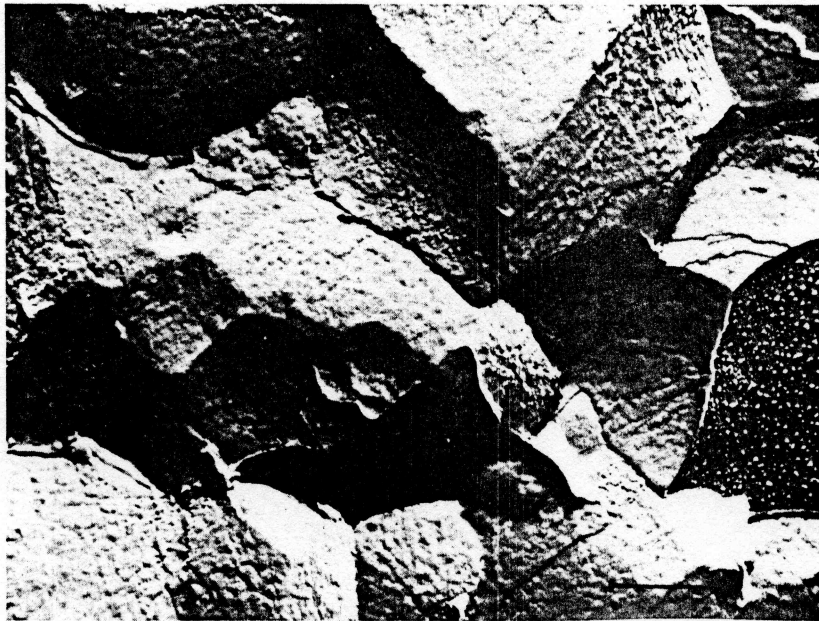


Fig. 21 Freeze-fracture electron micrograph of the above system at 30,000X.

Figure 22 shows the similarity between coacervation of a micellar solution in the absence of oil and the formation of a middle phase microemulsion in the presence of oil. The lower part of Figure 22 shows the transition of a birefringent surfactant formulation to an isotropic coacervate phase upon addition of salt. On the other hand, the same formulation in the presence of an equal volume of dodecane shows the formation of lower phase, middle phase and upper phase microemulsions. We propose that the middle phase microemulsion is similar to the coacervated phase containing some solubilized oil. Additional studies in support of these models have been reported elsewhere (21, 23, 24).

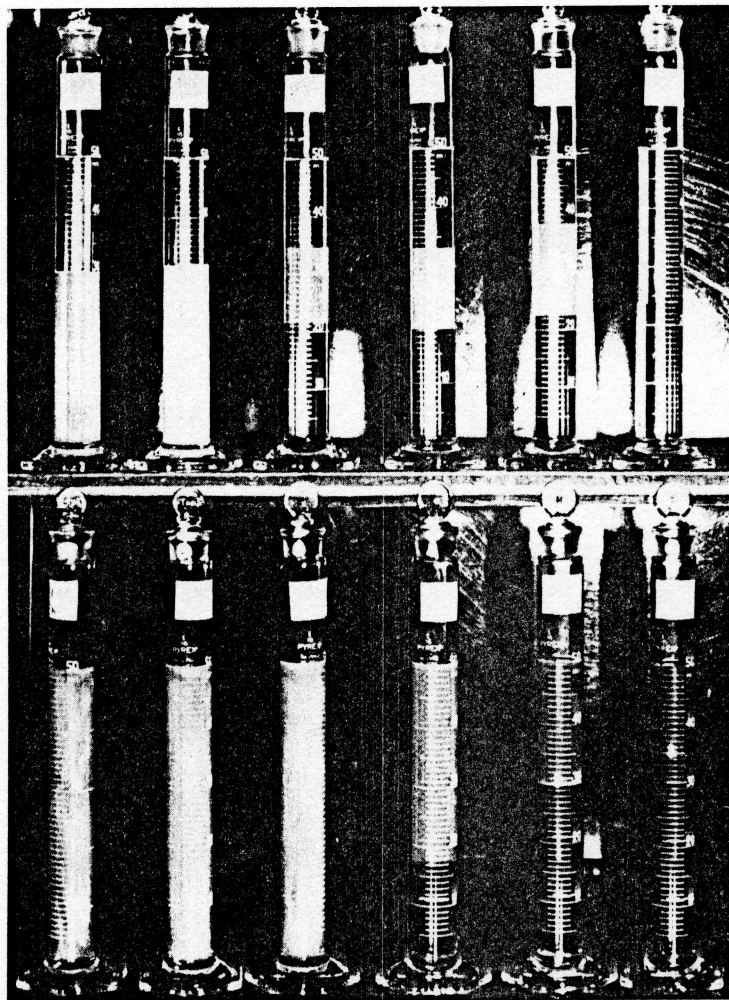


Fig. 22 A comparison of coacervation in aqueous solution with middle phase formation in surfactant/oil/brine/alcohol systems.

Figure 23 schematically shows the mechanism of formation of middle phase microemulsions as salinity is increased.

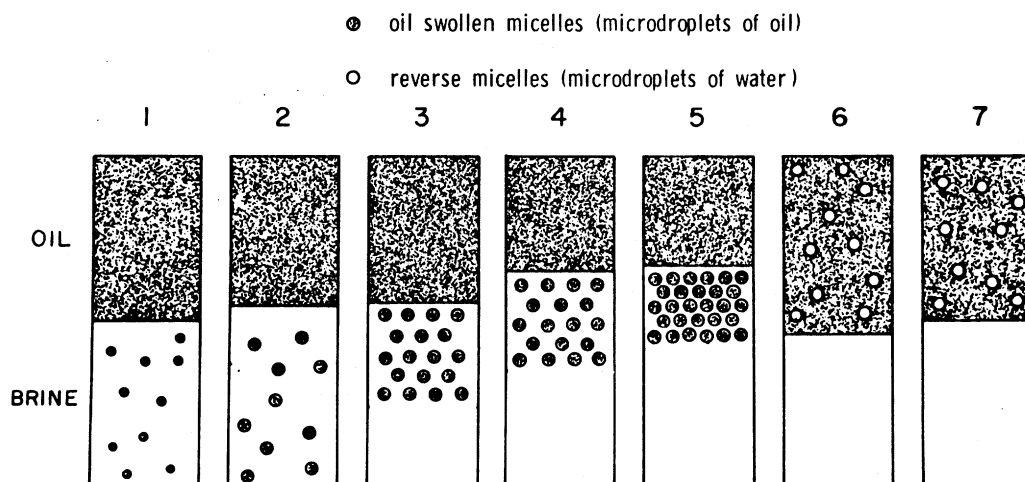


Fig. 23 A schematic illustration of the $1+m+u$ transition for the TRS 10-410/Isobutanol/Oil/Brine System.

As one increases the salinity, the cmc decreases, the aggregation number of the micelles increases and the solubilization of oil within micelles increases. The compression of the electrical double layer around micelles will occur, hence reducing the repulsive forces between the micelles. Thus the reduction in the repulsive forces and increase in the attractive forces between the micelles will bring the micelles closer and ultimately lead to a separation of a micelle rich phase forming the middle phase microemulsion. Upon further increase in salinity, the solubilization of oil in this middle phase increases whereas that of brine decreases. The magnitude of interfacial tension of the middle phase with oil or brine depends upon the extent of solubilization of oil and brine in the middle phase. In general, the higher the solubilization of oil or brine in the middle phase microemulsion, the lower is the interfacial tension with respect to these excess phases (28). The salinity at which equal volumes of oil and brine are solubilized in the middle phase microemulsion is referred to as optimal salinity for the surfactant-oil-brine systems under given physical chemical conditions (29, 30).

Figure 24 shows the freeze-fracture electron micrograph of a middle phase microemulsion formed in the system extensively studied by Reed and Healy (28-30).

It clearly shows the discrete spherical structures embedded in a continuous aqueous phase consistent with the mechanism proposed in Figure 23. It should be pointed out that other investigators (40-47) have proposed the possibility of bicontinuous structure or the coexistence of oil external and water external microemulsions in the middle phase. In very high surfactant concentration systems, (15-20%) the existence of anomalous structure which are neither conventional water external or oil external microemulsions have been proposed to account for some unusual properties of these systems (43-46).

Figure 25 shows that the transition $1+m+u$ is not only achieved by increasing the salinity but is also possible by changing any of the other 8 variables.

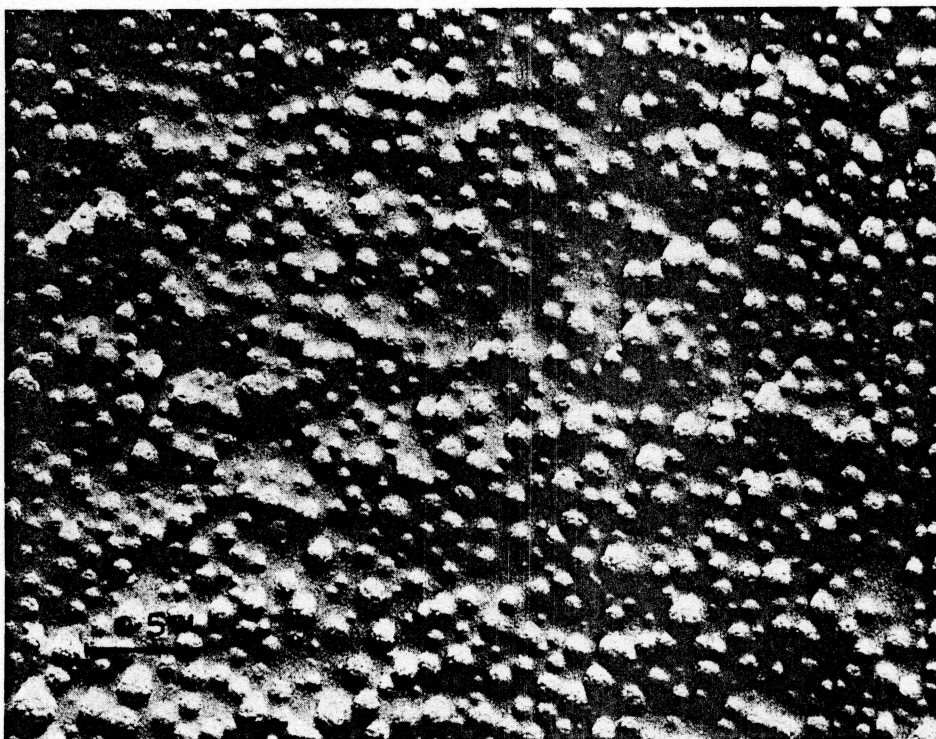
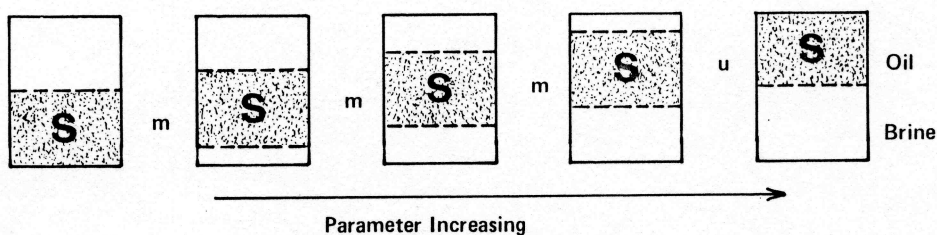


Fig. 24 Freeze-fracture electron micrograph of the middle phase of the Exxon system at the optimal salinity.



The transition $l \rightarrow m \rightarrow u$ occurs by:

1. Increasing Salinity
2. Decreasing oil chain length
3. Increasing alcohol concentration (C_4, C_5, C_6)
4. Decreasing temperature
5. Increasing total surfactant concentration
6. Increasing brine/oil ratio
7. Increasing surfactant solution/oil ratio
8. **Increasing molecular weight of surfactant**

Fig. 25 Schematic illustration of the factors influencing the $l \rightarrow m \rightarrow u$ transition in surfactant/oil/brine/alcohol systems.

Thus, by choice of a suitable parameter, one can obtain the transition in the structure of these microemulsions. At optimal salinity, the partition coefficient of surfactant in the excess oil and brine phases is found to be near unity and the interfacial tension between the excess oil and excess brine is also minimum (19).

The importance of the optimal salinity concept for enhanced oil recovery is shown in the data illustrated in Figure 26.

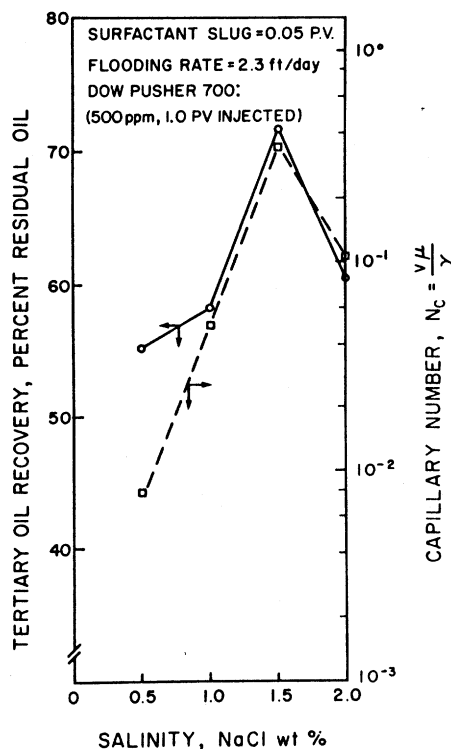


Fig. 26 Effect of salinity on the capillary number and tertiary oil recovery in sand packs.

It is evident that the oil recovery is maximum at optimal salinity for the systems reported here. An excellent correlation between the capillary number and oil recovery is also evident from Figure 26 (48). In view of this observation, the surfactant formulation for a practical application should be designed such that the reservoir salinity becomes the optimal salinity under the given reservoir conditions.

Figure 27 shows the effect of oil chain length on optimal salinity of the TRS 10-410 + isobutanol systems (49) and the corresponding interfacial tension at the optimal salinity for each oil chain length. It was observed that as the oil chain length increases, the optimal salinity increases and the volume of the middle phase decreases. The range over which the middle phase microemulsion exists also increases as the oil

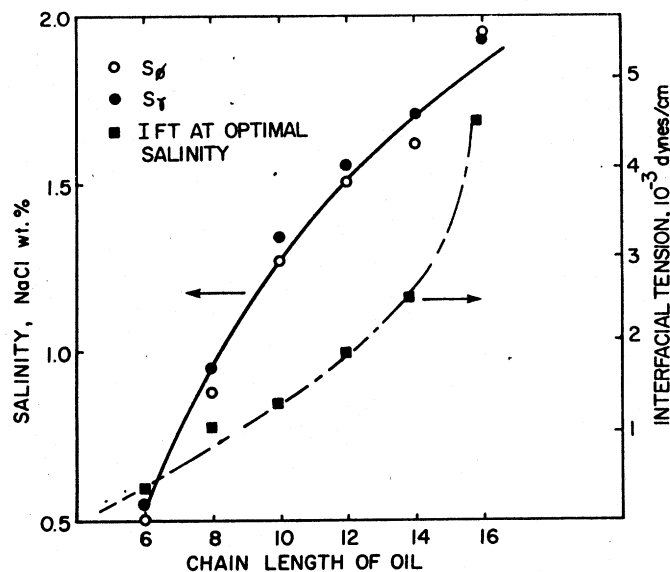


Fig. 27 Effect of oil chain length on the optimal salinity and interfacial tension at the optimal salinity.

chain length increases. It should be pointed out that from extensive studies on mixed alkanes, the concept of Equivalent Alkane Carbon Number (EACN) has been proposed to correlate the interfacial tension of pure alkanes with those of the mixtures (50). Many light crude oils have been simulated by the mixtures of pure hydrocarbons (51). Most light oils or the EACN for most light crude oils were found to be between C_7 and C_{11} .

Figure 28 shows the correlation of optimal salinity in the presence of various alcohols with their solubility in brine. Figure 28 summarizes the data obtained by three research groups (49,52, 53). It is interesting that the optimal salinity of a given oil and surfactant formulation lies near the intersection of the brine solubility. This correlation suggests that if one determines the optimal salinity in the presence of 2 or 3 alcohols, one can predict the optimal salinity in the presence of other alcohols from their brine solubility data. This is a very useful correlation and eliminates the time consuming and laborious procedure of obtaining the optimal salinity in the presence of each alcohol.

E. TRANSIENT PROCESSES

There are several transient processes, such as the formation and coalescence of drops as well as their flow through porous media, that are likely to occur in the surfactant-polymer flooding process. Figure 29 shows the coalescence or phase separation time of handshaken and sonicated macroemulsions as a function of salinity.

Surfactant: 50% TRS 10-410
 Alcohol: 3.0%
 Brine: Variable NaCl
 Oil: Dodecane
 WOR: 1.0
 Ref: Shah and Hsieh, SPE 6594
 4.0% Amoco AA-Sulfonate
 0.7%
 Variable NaCl
 Wyoming Crude Oil
 1.0
 Salter, SPE 6843
 1.5% Xylene Sulfonate
 0.5%
 Variable NaCl
 90/10 Isopar M/HAN
 1.0
 Puerto and Gale, SPE 5814

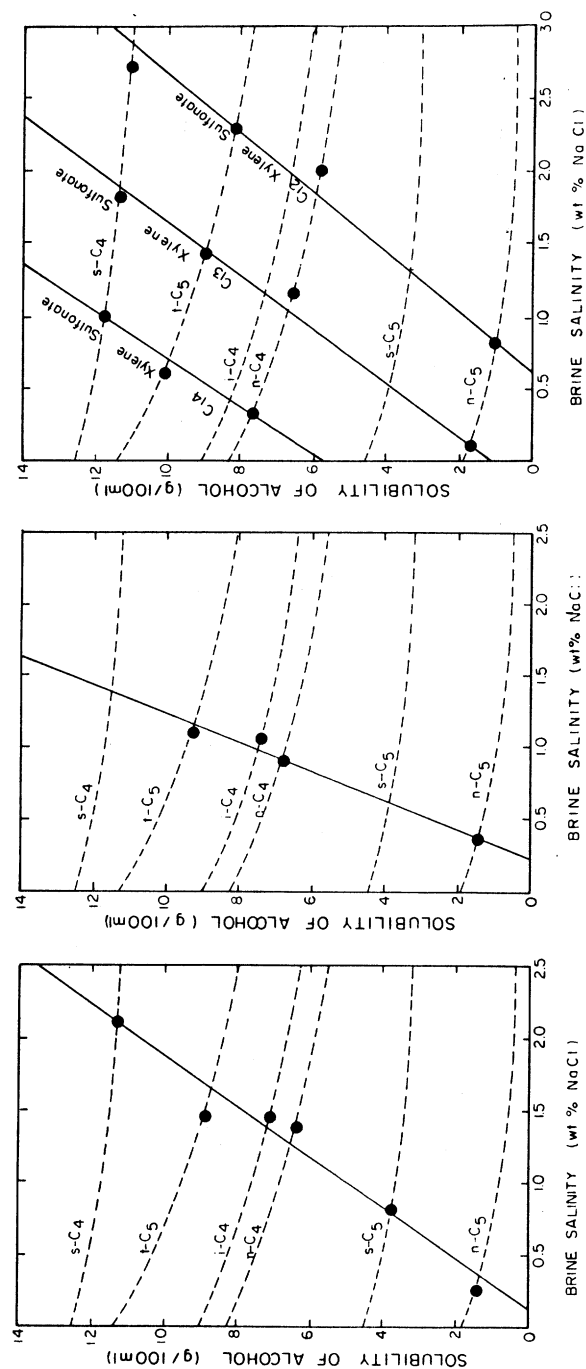


Fig. 28 A correlation of optimal salinity in the presence of various alcohols with their solubility in brine.

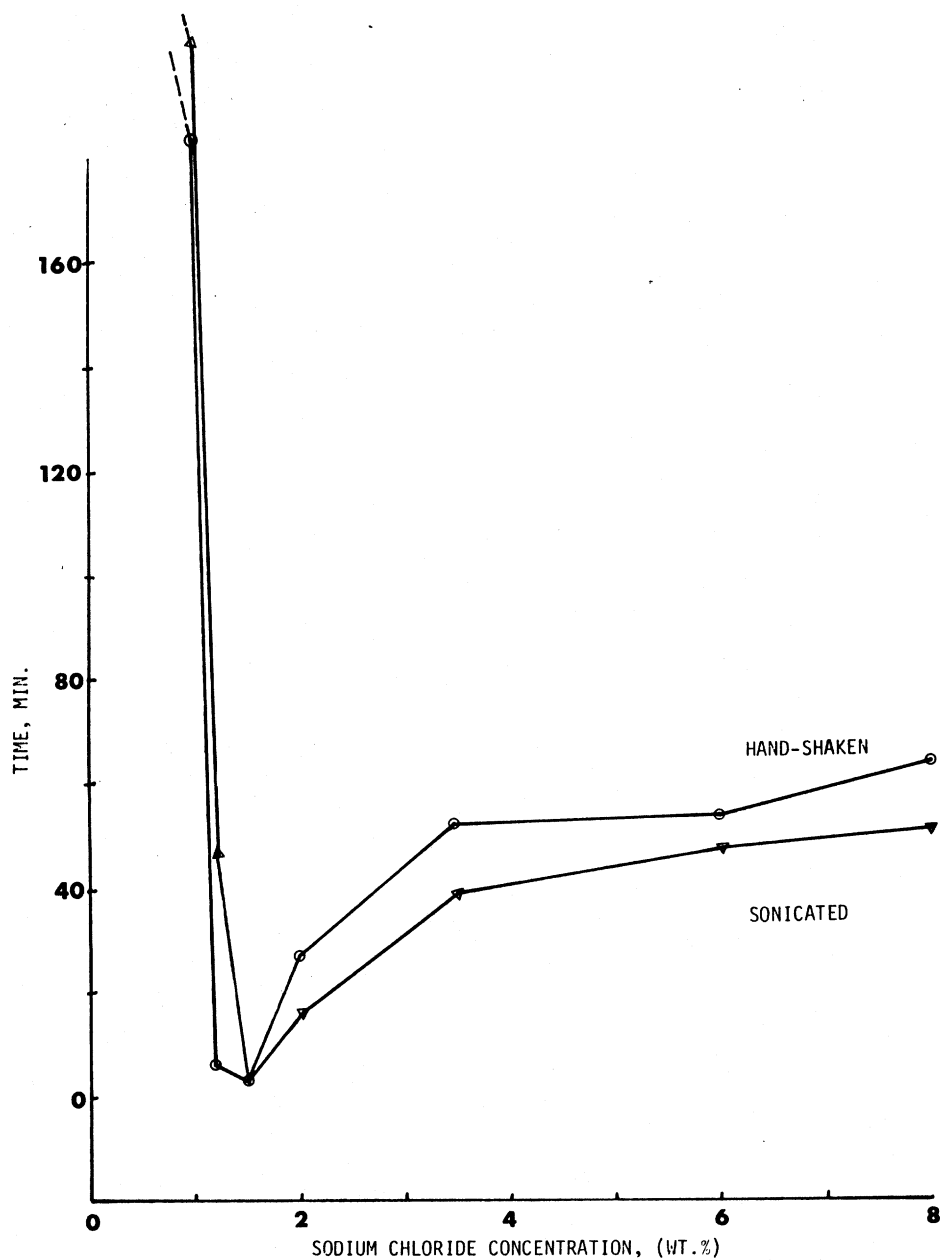


Fig. 29 Effect of salinity on the phase separation or coalescence rate of sonicated and hand-shaken emulsions.

It is obvious that minimal phase separation time or the fastest coalescence rate occurs at the optimal salinity (54). The rapid coalescence could contribute significantly to the formation of an oil bank from the mobilized oil ganglia. This also suggest that at the optimal salinity the interfacial viscosity must be very low to promote the rapid coalescence.

Figure 30 shows the pressure drop across a porous medium when emulsions prepared at various salinities flow through it. It is evident that the minimum pressure drop occurs at and around the optimal salinity of the surfactant formulation. This also suggests that the interfacial tension is an important factor influencing the pressure drop across porous media (54).

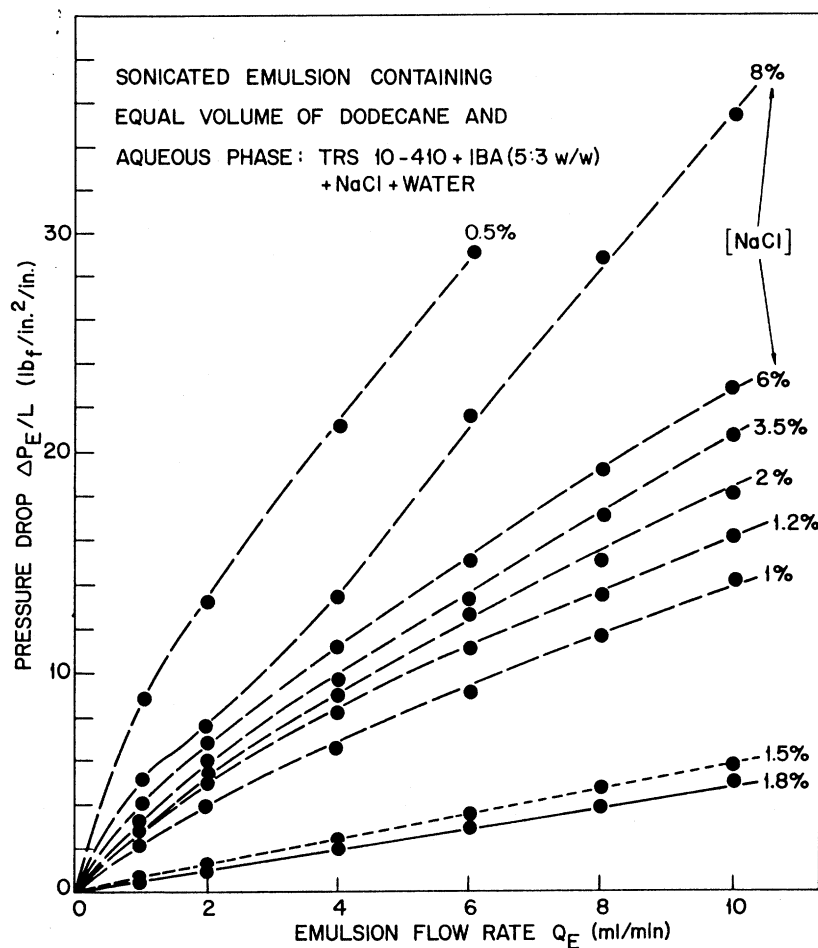


Fig. 30 Effect of salinity on the pressure drop-flow rate curves of sonicated emulsions.

Figure 31 shows a very interesting and important correlation between the coalescence rate in emulsions and the apparent viscosity in the flow through porous media. The minimum apparent viscosity for the flow of emulsions in porous media coincides with minimum phase separation time at the optimal salinity.

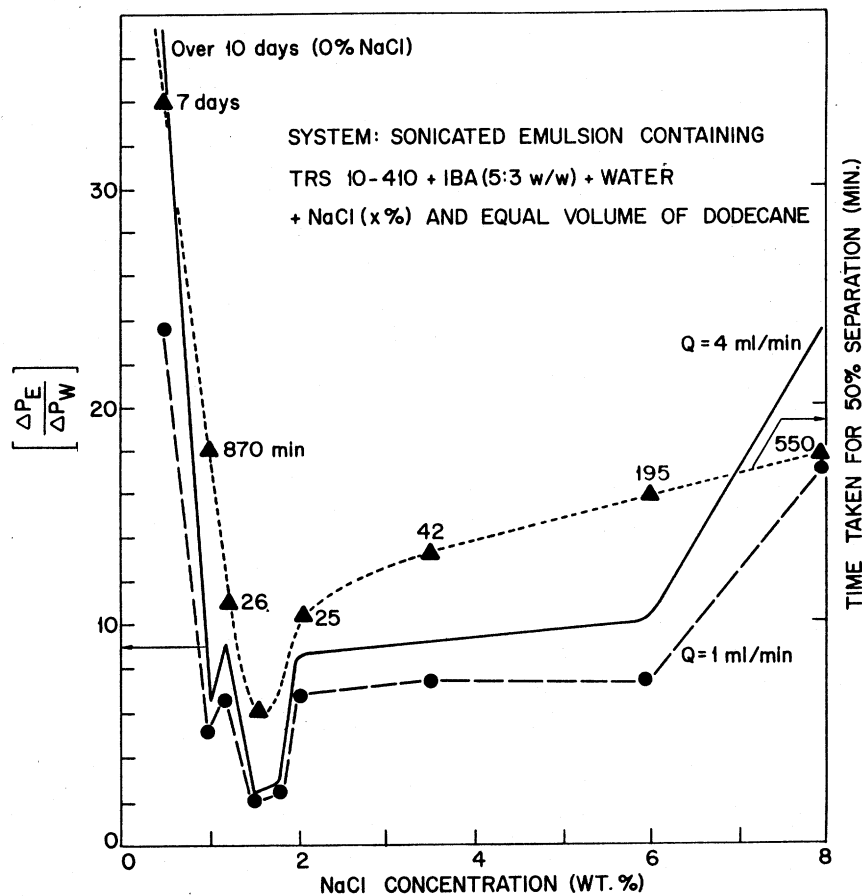


Fig. 31 A correlation between the apparent viscosity and coalescence rate of sonicated emulsions.

This correlation between the phenomena occurring in porous media and outside the porous medium allows us to use coalescence measurements as a screening criterion for many surfactant formulations for their possible behavior in porous media. It is likely that a rapidly coalescing emulsion will give a lower apparent viscosity for the flow in porous media (54).

Figure 32 summarizes all the phenomena occurring at the optimal salinity in relation to enhanced oil recovery by surfactant-polymer flooding.

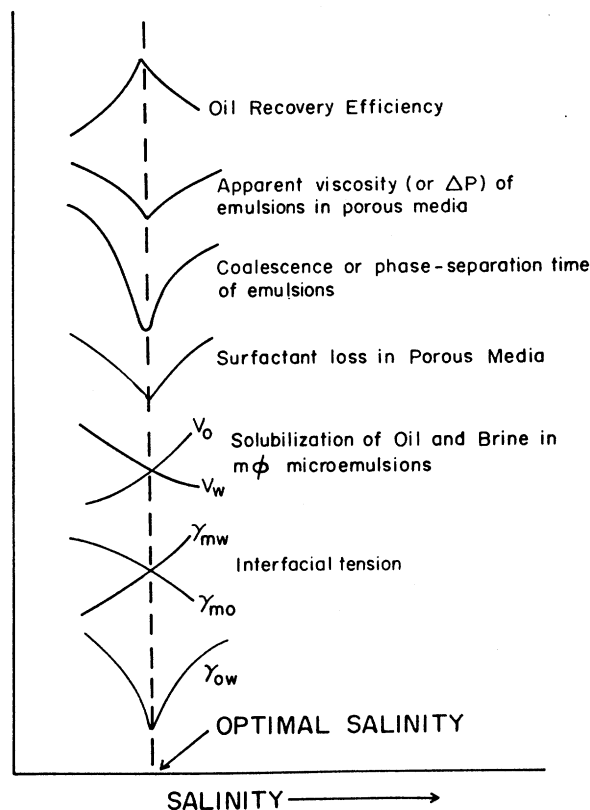


Fig. 32 A summary of various phenomena occurring at the optimal salinity in relation to enhanced oil recovery by surfactant-polymer flooding.

It is evident that the maximum in oil recovery efficiency correlates well with transient and equilibrium properties of surfactant-oil-brine systems. In our preliminary studies, we have found that the surfactant loss in porous media is also minimum at the optimal salinity presumably due to reduction in the entrapment process for the surfactant phase. Therefore, the maximum in oil recovery at optimal salinity might be a combined effect of all these processes taking place at the optimal salinity.

Since optimal salinity leads to favorable conditions for optimal oil recovery, one would like to design approaches to alter the optimal salinity of a given surfactant formulation (55-57). Figure 33 shows the optimal salinity of a mixed surfactant formulation consisting of a petroleum sulfonate and ethoxylated sulfonate (EOR-200).

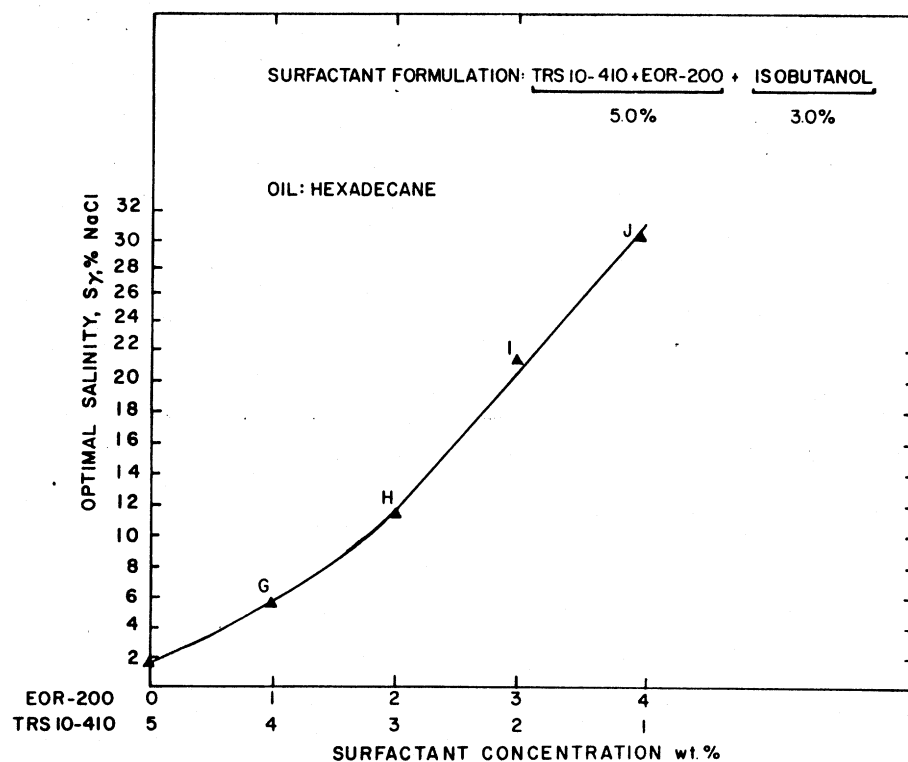


Fig. 33. Increase in the optimal salinity of surfactant formulation by addition of EOR-200.

As one replaces petroleum sulfonates with the ethoxylated sulfonate the optimal salinity increases and can reach as high as 32% NaCl brine. Interestingly, these formulations when equilibrated with oil produced middle phase microemulsions having very low interfacial tension. Thus, the mixed surfactant formulations containing petroleum sulfonates and ethoxylated sulfonates or alcohol are promising candidates for high salinity formulations (55,56).

Figure 34 shows the shape of an oil drop upon contacting a surfactant formulation consisting of 0.05% TRS 10-80 in 1% NaCl. It is evident that as surfactant molecules migrate from the aqueous phase to the interface and subsequently to the oil phase the interfacial tension decreases and the spherical drop gradually flattens out. This flattening

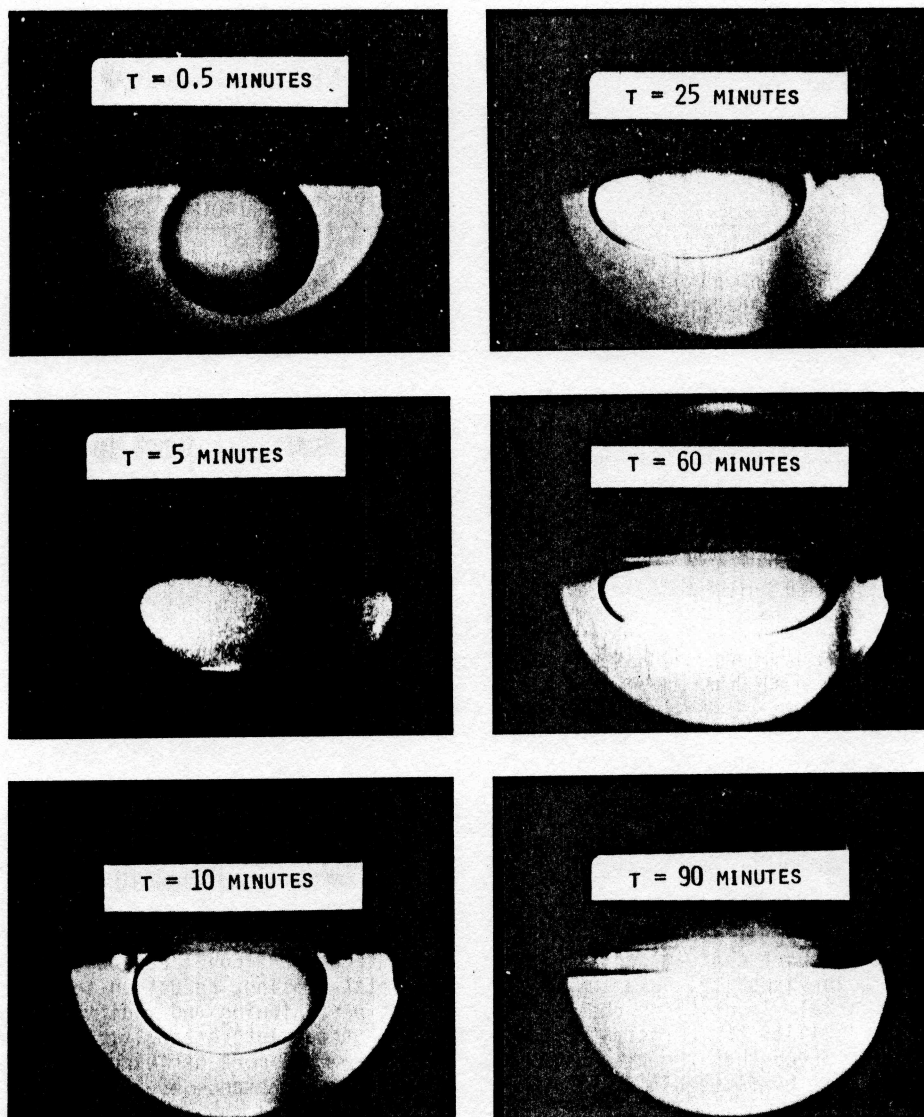


Fig. 34. An illustration of the drop flattening phenomenon for a drop of octane in an equilibrated solution of 0.05% TRS 10-80 in 1% NaCl.

time reflects the rate at which molecules accumulate at the oil-brine interface. As shown in Table 1, there is a good correlation between the flattening time, IFT and the oil recovery. The reduction in the flattening time leads to favorable oil recovery efficiency (16,48).

TABLE 1

IFT, Flattening Time and Oil Recovery Efficiency of 0.05% TRS 10-80 in 1% NaCl vs. n-Octane at 25°C

| SYSTEM | IFT (mN/m) | FLATTENING TIME* (seconds) | OIL RECOVERY* (% OIP) |
|--|---------------------|-------------------------------|--------------------------|
| I. Fresh Oil/1% NaCl | $\approx 50.8^{**}$ | ∞ | 61-63 |
| II. Fresh Oil/Equilibrated Surfactant Solution | 0.731 | 6600 | 44-52 |
| III. Fresh Oil/Fresh Surfactant Solution | 0.627 | 480 | 75-77 |
| IV. Equilibrated Oil/% NaCl | 0.121 | 900 | 83 |
| V. Equilibrated Oil/Equilibrated Surfactant Solution | 0.0267 | 240 | 94 |
| VI. Equilibrated Oil/Fresh Surfactant Solution | 0.00209 | 15 | - |

*Flattening time is defined as the time required for the n-octane drop to gradually flatten out.

**Octane/H₂O, 20°C, IFT = 50.8 mN/m, "Interfacial Phenomena", Davies and Rideal, Chapter I, p. 17 Table I, Academic Press, N.Y. 1963.

+ Sandpack dimensions: 1.06" dia. x 7" long; Permeability= 3 darcy; flow rate: 2.3 ft./day.

In general, a surfactant formulation for enhanced oil recovery includes a short chain alcohol. The possible effect of alcohol can be the change in viscosity, lowering of the interfacial tension, reduction in interfacial viscosity or change in surfactant partitioning and modifying the solubility of surfactant in oil or brine phase. Interestingly, we have observed that the presence of alcohol has a much more striking effect on the flattening time of an oil drop in the presence of a surfactant formulation. As shown in Table 2 it compares the many interfacial properties, flattening time and oil recovery efficiency in the presence and absence of alcohol (16). It is evident that the flattening time decreases strikingly in the presence of alcohol suggesting that the alcohol promotes the mass transfer to the interface and a rapid reduction in the magnitude of the interfacial tension.

There are also time dependent changes in the surface properties of a surfactant formulation. This include the chemical degradation (58,59), or changes in the aggregation process of micelles (60). Several investigators have shown that the interfacial tension changes with time (61). We have also shown that using several physical techniques that molecular association also changes with time leading to the aging effects of the surfactant formulation (58). The aging processes may occur over a period of months or years.

Table 2

The Effect of IBA on Flattening Time,
IFT, IFV, Partition Coefficient, and Oil
Displacement Efficiency

| <u>SYSTEM</u> | 0.1% TRS 10-410 in 1.5% NaCl vs. n-Dodecane | 0.1% TRS 10-410 + 0.06% IBA in 1.5% NaCl vs. n-Dodecane | 0.05% TRS 10-80 in 1% NaCl vs. n-Octane | 0.05% TRS 10-80 + 0.04% IBA in 1% NaCl vs. n- Octane |
|---|---|---|---|---|
| <u>Run</u> | S100-48 | S100-43 | S100-02 | S100-44 |
| <u>Flattening Time</u> | 90 sec | < 1 sec | 420 sec | < 1 sec |
| <u>IFT (dynes/cm)</u> | 0.086 | 0.088 | 0.025 | 0.024 |
| <u>Interfacial Viscosity (s.p.)</u> | 0.096 | 0.086 | 0.023 | 0.018 |
| <u>Partition Coefficient</u> | 0.010 | 0.009 | 0.3 | 1.36 |
| <u>Secondary Recovery</u> | | | | |
| <u>By Brine Flooding</u> | - | - | 61.2% | 60.08% |
| <u>By Surfactant Soln Flooding</u> | 84.37% | 98.32% | 60% | 91% |
| <u>Tertiary Recovery</u> | - | - | 0 | 76.84% |
| <u>Final Oil Saturation</u> | 11.73% | 1.28% | 30% | 5.36% |

*All displacement experiments are carried out with nonequilibrated systems in sand packs at 25°C; Dimensions and flow rates same as given in Table 2.

Secondary and tertiary oil recovery values are percent of oil-in-place, whereas final oil saturation is percent of total pore volume.

F. SURFACTANT-POLYMER INCOMPATIBILITY

Trushenski (17) has shown that surfactant-polymer incompatibility can lead to a considerable reduction in the efficiency of the process. The surfactant-polymer incompatibility manifests itself as a phase separation and alteration of the viscosity of the separated phases. The entrapment of the high viscosity phase will effectively remove that component from the flooding process. The mixing of the surfactant and polymer in the porous medium occurs due to both dispersion effects as well as excluded volume effects for the flow of polymer molecules in porous media.

Figure 35 shows the effect of mixing surfactant and a polymer solution in the absence of oil.

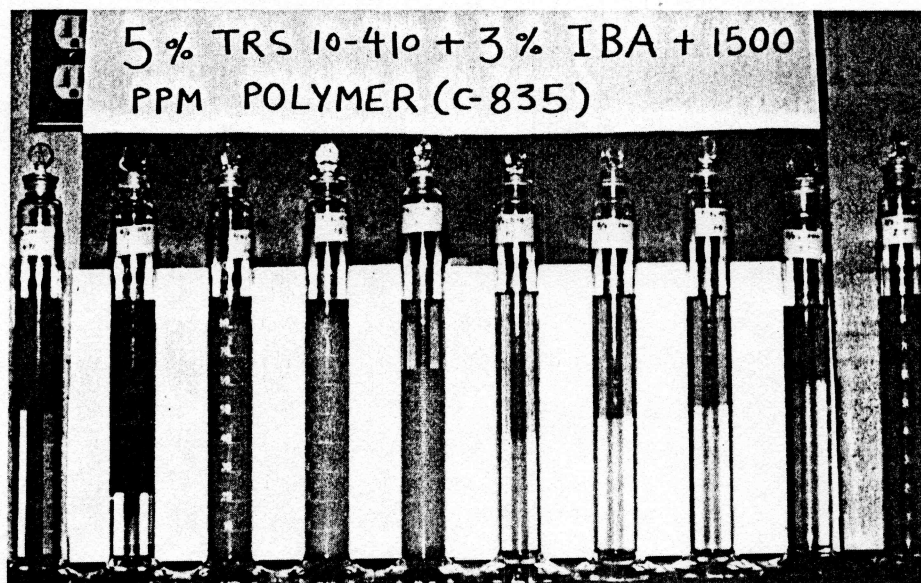


Fig. 35. Effect of addition of polymer on the phase behavior of aqueous surfactant solutions.

It is evident that there are two regions of phase separation, one at low salinity and the other at high salinity separated by a metastable colloidal dispersion. We refer to the separation at the lower salinity as region 1 and those at high salinity as region 2. The separation of a surfactant-rich phase in region 2 is similar to that in coacervation process, whereas the separation of micelles in region 1 is induced by the presence of polymer molecules. The surfactant-polymer incompatibility shows up strikingly in the formation of region 1 (62).

The addition of polymer to an oil/brine/surfactant/alcohol system shows that the formation of middle phase microemulsion is promoted by the presence of polymer (Figure 36). However, the transition middle phase to upper phase microemulsion is not influenced at all by the presence of polymer. We have further shown (62,63) that the optimal salinity is not significantly influenced by the presence of polymer in the oil/brine/surfactant/alcohol system.

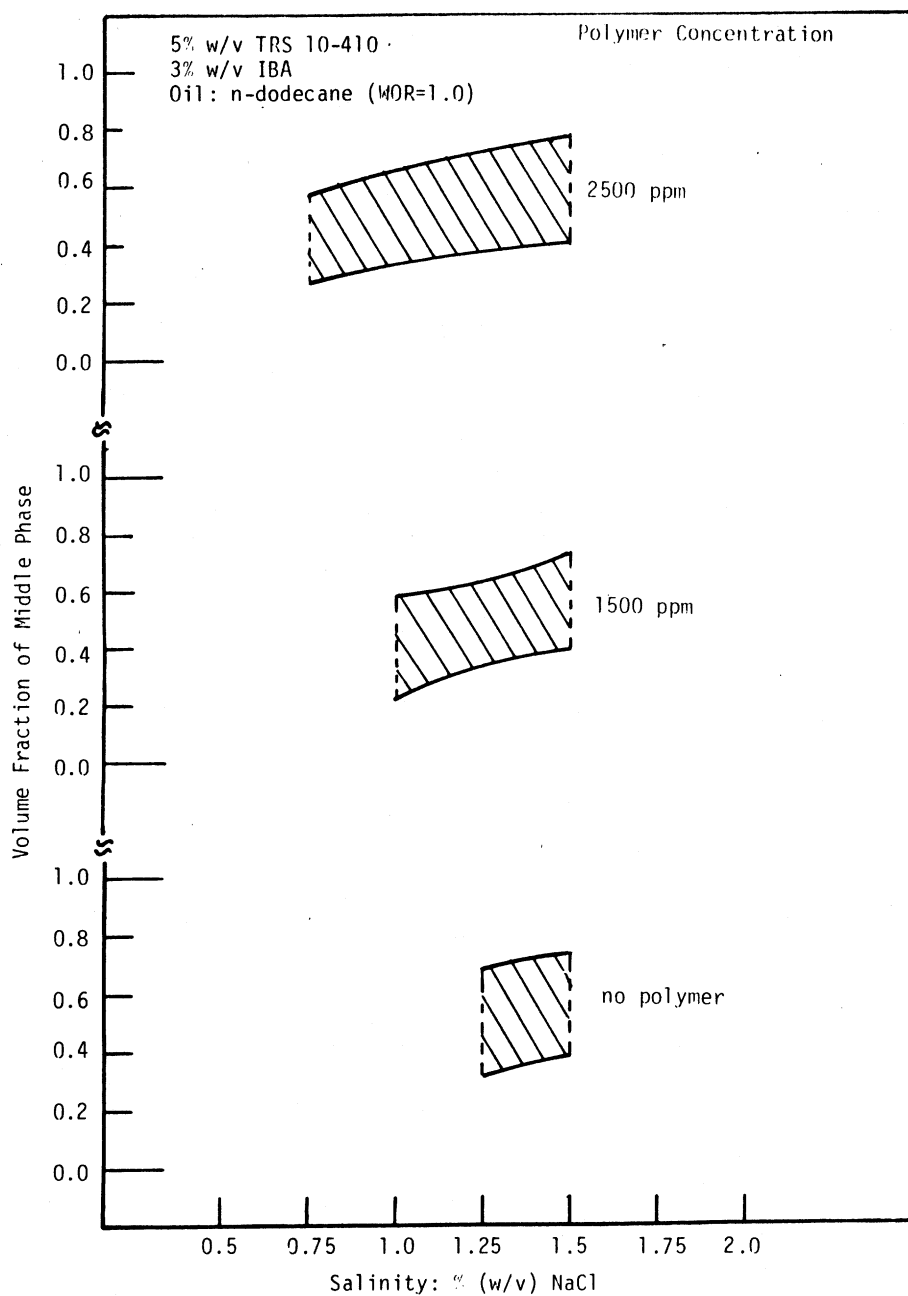


Fig. 36. Effect of polymer concentration on the salinity range for formation of middle-phase microemulsion.

Figure 37 shows the schematic explanation of the surfactant polymer incompatibility and concomitant phase separation.

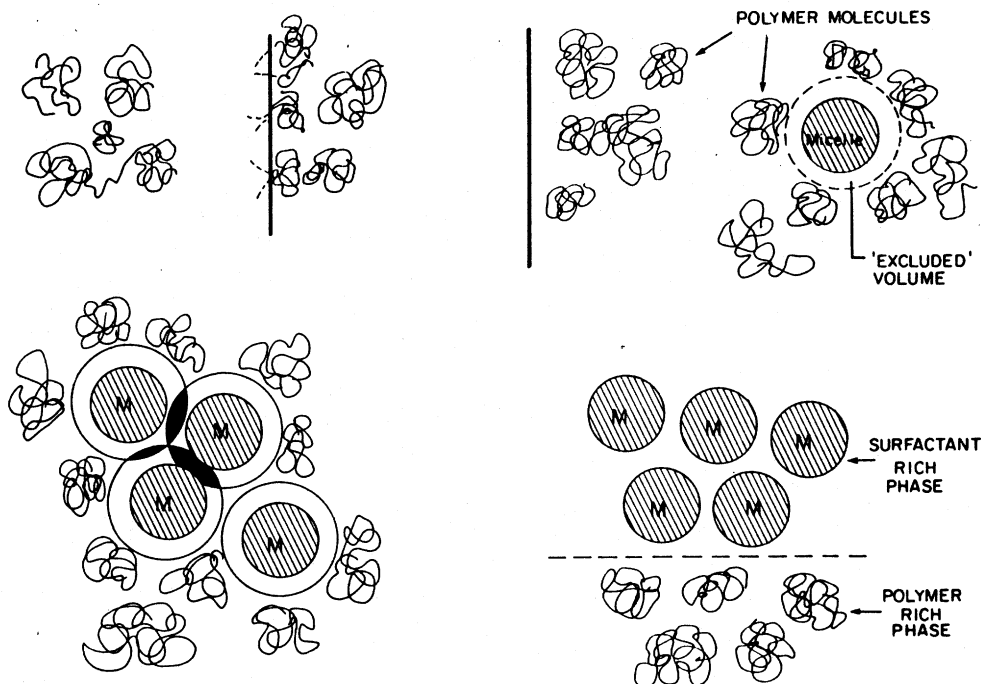


Fig. 37. Schematic illustration of surfactant-polymer incompatibility leading to phase separation in mixed surfactant-polymer systems.

We propose that around each micelle there is a region of solvent that is excluded to polymer molecules. However, when these micelles approach each other there is overlapping of this excluded region. Thus if all micelles separate out then the excluded region diminishes due to the overlap of the shell and more solvent becomes available for the polymer molecules. This effect is similar to what is called polymer depletion stabilization (61). Thus in a way, this is similar to osmotic effect where the polymer molecule tends to maximize the solvent for all possible configurations.

G. NEW CONCEPTS IN EOR PROCESS DESIGN

The formation of an oil bank is a very important event in the surfactant-polymer flooding process. This was established from studies on the injection of an artificial oil bank followed by the surfactant formulation that can produce ultralow IFT with the injected oil. We found that the oil recovery increased substantially and the residual oil saturation decreased with the injection of oil bank as compared to the same studies carried out in the absence of an injected oil bank (48).

Figure 38 schematically shows that the oil bank formation and its propagation is analogous to "snowball effect".

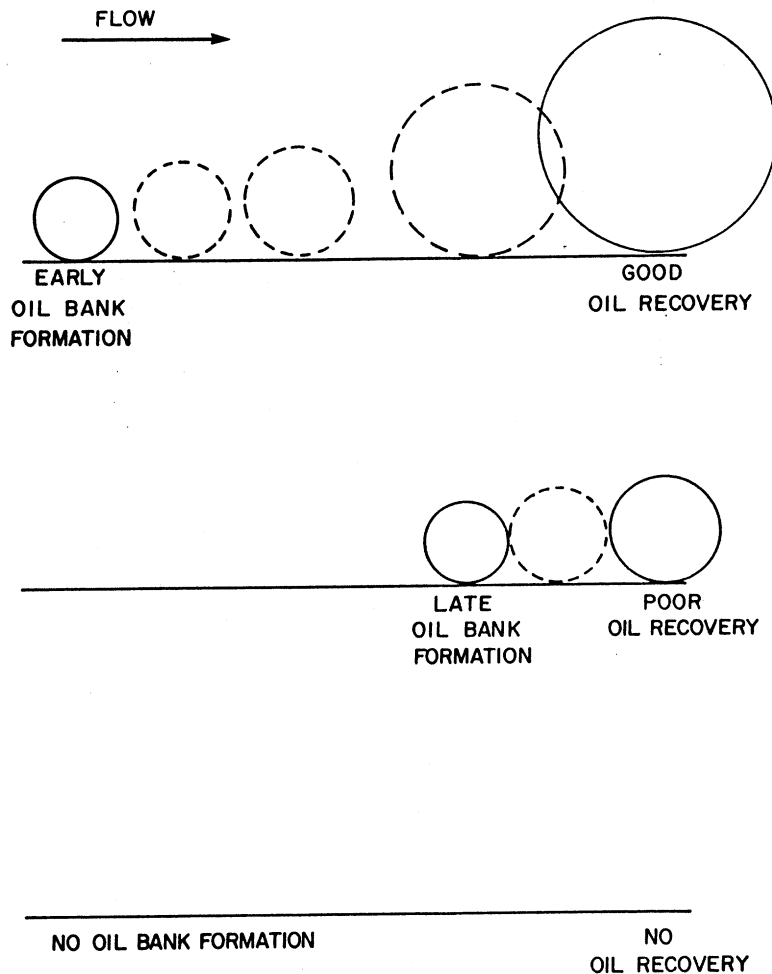


Fig. 38. Schematic illustration of the injection of an oil bank and the subsequent "snowball effect" in enhanced oil recovery.

If an early oil bank forms as it moves through the porous medium, it accumulates additional oil ganglia resulting in an excellent oil recovery whereas a late oil bank formation will result in a poor oil recovery.

We have shown that the salinity of polymer solution is far more important than the salinity of connate water (23). When the salinity of polymer solution was at the optimal salinity of the surfactant formulation, high oil recovery efficiency was obtained over a wide range of connate water salinities. Evidence showed that the phase behavior of the

surfactant slug in porous media is largely determined by the salinity of the polymer solution (65). For better mobility control and minimal surfactant loss a two-slug design of a surfactant formulation was employed (23). In this design, the first surfactant slug has an optimal salinity close to the connate water salinity and the second surfactant slug has a much lower optimal salinity. The polymer solution salinity is made equal to the optimal salinity of the second surfactant slug. With this design, high oil recovery in Berea cores can be obtained even in the presence of high salinity (6% NaCl + 1% calcium chloride) connate water.

The optimal salinity concept is further extended to include the effect of mobility control and surfactant dispersion and entrapment in porous media (65). The proposed salinity shock design of mobility polymer solutions employs two slugs of polymer solutions in which the first polymer slug is at the optimal salinity of the preceding surfactant formulation and the second polymer slug is at a much lower salinity.

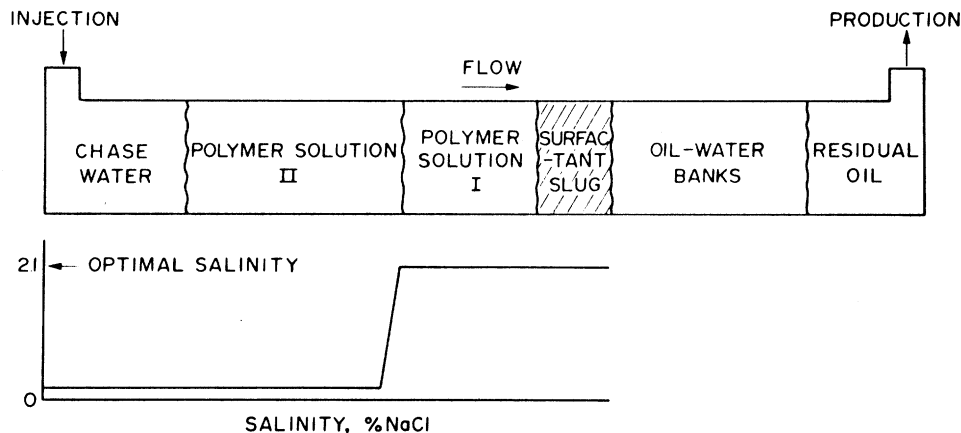


Fig. 39. Schematic representation of the graded-salinity design of polymer buffer solution for enhanced oil recovery.

With this unique design high oil recovery and high surfactant recovery can be obtained for soluble oil flooding in sandpacks, while the polymer consumption can be greatly reduced.

Figure 40 schematically shows our results obtained using the salinity shock design. The optimal salinity for the surfactant formulation used was 2.1% NaCl and the reservoir brine was 3% NaCl plus 1% calcium chloride. By the use of two polymer slugs we were able to obtain in Berea cores 88% tertiary oil recovery and 48% surfactant recovery.

For aqueous micellar-polymer flooding with crude oil in Berea cores, it has been shown (66-69) that a contrast salinity design of the preflush micellar-polymer flooding process may produce a better oil recovery than that obtained from a constant salinity process. In the contrast salinity design, the salinity of the preflush water is made higher while the salinity of the polymer solution is made lower than the optimal salinity of the surfactant formulation. The rationale of this design is that an optimal salinity profile can be established in the vicinity of the surfactant slug upon mixing of the injected fluids in the porous medium.




| | | SOLUBLE OIL | | CONNATE WATER | |
|-----|-------------|--------------------------------|--|---------------------------------|--|
| I | CHASE WATER | POLYMER SLUG 2.1% NaCl |  OIL-WATER BANK | 3% NaCl 1% CaCl ₂ | |
| | | TERTIARY OIL RECOVERY 51 % | | SURFACTANT RECOVERY 7 % | |
| II | CHASE WATER | POLYMER SLUG 0.05 % NaCl |  OIL-WATER BANK | 3% NaCl 1% CaCl ₂ | |
| | | 42 % | | 25 % | |
| III | CHASE WATER | POLYMER SLUG II 0.05 % NaCl | POLYMER SLUG I 2.1 % NaCl  OIL-WATER BANK | 3% NaCl 1% CaCl ₂ | |
| | | 88 % | | 48 % | |

Fig. 40. The effect of salinity shock of polymer buffer solution on oil displacement efficiency and surfactant loss.

It is hoped that the experimental results presented in this paper contribute in a small way to increasing our understanding of phenomena occurring in porous media. It should be emphasized that results we have obtained using laboratory scale experiments are neither conducted nor intended to be extrapolated to the oil field processes. It is recognized that the processes occurring in petroleum reservoirs are far more complex than those that we can design and control using a laboratory setup.

ACKNOWLEDGEMENTS

The author wishes to express his sincere thanks and appreciation to the National Science Foundation - RANN, ERDA and the Department of Energy (Grant No. DE-AC1979BC10075) and the consortium of the following Industrial Associates for their generous support of the University of Florida Enhanced Oil Recovery Research Program during the past seven years: 1) Alberta Research Council, Canada, 2) American Cyanamid Co., 3) Amoco Production Co., 4) Atlantic-Richfield Co., 5) BASF-Wyandotte Co., 6) British Petroleum Co., England, 7) Calgon Corp., 8) Cities Service Oil Co., 9) Continental Oil Co., 10) Ethyl Corp., 11) Exxon Production Research Co., 12) Getty Oil Co., 13) Gulf Research and Development Co., 14) Marathon Oil Co., 15) Mobil Research and Development Co., 16) Nalco Chemical Co., 17) Phillips Petroleum Co., 18) Shell Development Co., 19) Standard Oil of Ohio Co., 20) Stepan Chemical Co., 21) Sun Oil Chemical Co., 22) Texaco, Inc., 23) Union Carbide Corp., 24) Union Oil Co., 25) Westvaco, Inc., 26) Witco Chemical Co., and the University of Florida. He also wishes to convey his sincere thanks to his colleagues in Chemical Engineering, Petroleum Engineering and Institute for Energy Studies of Stanford University for their collaboration during his stay at Stanford University.

REFERENCES

1. "Improved Oil Recovery by Surfactant and Polymer Flooding", D.O. Shah and R.S. Schechter eds., Acad. Press, Inc., N.Y. (1977).
2. "Surface Phenomena in Enhanced Oil Recovery", D.O. Shah, ed. Proceedings of the Symposium on Enhanced Oil Recovery, Stockholm, Sweden, Aug. 20-25, 1979, Plenum Publishing Company, N.Y. (in press).
3. "SPE Improved Oil Recovery Reprints," Proceedings of Symposium on Improved Oil Recovery, Tulsa, OK., April 16-19, 1972.
4. "Proceedings of the SPE-AIME Symposium on Improved Oil Recovery", Tulsa, OK, April 22-24, 1974.
5. "Proceedings of the SPE-AIME Symposium on Improved Oil Recovery", Tulsa, OK, March 22-24, 1976.
6. "Proceedings of the SPE-AIME Symposium on Improved Oil Recovery", Tulsa, OK, April 16-19, 1978.
7. "Proceedings of the SPE International Symposium on Oilfield and Geothermal Chemistry," Houston, TX, Jan. 22-24, 1979.
8. "Proceedings of the SPE-AIME Symposium on Improved Oil Recovery", Tulsa, OK, April 20-23, 1980.
9. "Proceedings of the European Symposium on Enhanced Oil Recovery, Edinburgh, Scotland, July 5-7, 1978.
10. "Proceedings of the 1980 SPE International Symposium on Oilfield and Geothermal Chemistry, Stanford, CA., May 28-30, 1980.
11. "Secondary and Tertiary Oil Recovery Processes," Interstate Oil Compact Commission, Oklahoma City, OK (1974).
12. Taber, J.J., "Research on Enhanced Oil Recovery: Past, Present and Future" in "Surface Phenomena in Enhanced Oil Recovery", pp. 13-53, D.O. Shah, ed., Plenum Publishing Co., N.Y. (in press).
13. Foster, W.R., J. Pet. Tech., 25, 205 (1973).
14. Bansal, V.K. and Shah, D.O., in "Micellization, Solubilization, and Microemulsions", Vol. I pp. 87-113, K.L. Mittal, ed., Plenum Press, N.Y. (1977).
15. Pasquarelli, C.H. and Wasan, D.T., in "Surface Phenomena in Enhanced Oil Recovery", pp. 237-248, D.O. Shah, ed., Proceedings of the Symposium on Enhanced Oil Recovery, Stockholm, Sweden, Aug. 20-25, 1979, Plenum Publishing Company, NY. (in press).
16. Chiang, M.Y. and Shah, D.O., "The Effect of Alcohol on Surfactant Mass Transfer across the Oil/Brine Interface and Related Phenomena," SPE 8988, presented at the SPE 5th Intl. Sympo. on Oilfield and Geothermal Chemistry, Stanford, CA, May 28-30, 1980.

17. Trushenski, S.P., in "Improved Oil Recovery by Surfactant and Polymer Flooding", D.O. Shah and R.S. Schechter, eds., Acad. Press, Inc., N.Y., (1977).
18. Chiang, M.Y., Chan, K.S. and Shah, D.O., J. Can. Pet. Tech., 17(4), 1 (1978).
19. Chan, K.S. Ph.D. Dissertation, University of Florida (1978).
20. Wade, W.H., Vasquez, E., Salager, J.L., El-Emory, M., Koukounis, C. and Schechter, R.S., in "Solution Chemistry of Surfactants", Vol. II, pp. 801-816, K.L. Mittal, ed., Plenum Press, N.Y. (1979).
21. Noronha, J.C., Ph.D. Dissertation, University of Florida (1980).
22. Chan, K.S. and Shah, D.O., J. Disp. Sci., Tech. 1(1), 55 (1980).
23. Chou, S.I., Ph.D. Dissertation, University of Florida, (1980).
24. Hsieh, W.C., Ph.D. Dissertation, University of Florida (1977).
25. Bansal, V.K., Chan, K.S. McCallough, R. and Shah, D.O., J. Can. Pet. Tech., 17(1), 1 (1978).
26. Shah, D.O., Chan, K.S. and Giordano, R.M., in "Solution Chemistry of Surfactants", Vol. I pp. 391-406, K.L. Mittal, ed., Plenum Press, N.Y. (1977).
27. Rashid, S.N., in "University of Florida Research on Surfactant-Polymer Oil Recovery Systems - Annual Report" pp. 11-14, Dec. 1979.
28. Robbins, M.L., "Theory of the Phase Behavior of Microemulsions", SPE 5839, presented at the SPE Improved Oil Recovery Symposium, Tulsa, OK March 22-24 (1976).
29. Healy, R.N. and Reed, R.L., SPE J., 491 (Oct. 1974).
30. Healy, R.N. and Reed, R.L., SPE J., 147 (June 1976).
31. Shah, D.O. and Hamlin, R.M. Jr., Science, 171, 483 (1971)
32. Shah, D.O., Tamjeedi, A., Falco, J.W. and Walker, R.D. Jr., AIChE J., 18(6) 1116 (1972).
33. Falco, J.W., Walker, R.D., Jr. and Shah, D.O., AIChE J., 20(3), 510 (1974).
34. Shah, D.O., Walker, R.D., Hsieh, W.C., Shah, N.J. Dwivedi, S., Nelander, J., Pepinsky, R. and Deamer, D.W., SPE 5815 presented at the SPE Improved Oil Recovery Symposium, Tulsa, OK, March 22-24, 1976.
35. Bansal, V.K., Chinnaswamy, K., Ramachandran, C. and Shah, D.O., J. Colloid Interface Science, 72(3), 524 (1979).
36. Bansal, V.K., Shah, D.O. and O'Connell, J.P., J. Colloid Interface Science, 75(2), 462 (1980)
37. Chou, S.I. and Shah, D.O., J. Colloid Interface Sci., 78(1), 249 (1980).

38. Chou, S.I. and Shah, D.O., J. Colloid Interface Sci., 80(1), 49 (1981).
39. Chou, S.I. and Shah, D.O., J. Colloid Interface Sci., 80(2), 311 (1981).
40. Scriven, L.E., Nature, 263, 123 (1976).
41. Scriven, L.E., in "Micellization, Solubilization and Microemulsions", ed. K.L. Mittal, Vol. II, pp. 877, Plenum Press, N.Y. (1977).
42. Ramachandran, C., Vijayan, S. and Shah, D.O., J. Phys. Chem., 84, 1561 (1980).
43. Hwan, R., Miller, C.A. and Fort, T. Jr., J. Colloid Interface Sci., 68, 221 (1979).
44. Shinoda, K. J. Colloid Interface Sci., 24, 4 (1967).
45. Shinoda, K. and Saito, H., J. Colloid Interface Sci., 26, 70 (1968).
46. Friberg, S., Lapczynska, I. and Gilberg, G., J. Colloid Interface Sci., 56, 19 (1976).
47. Miller, C.A., Hwan, R., Benton, W.J. and Fort, T. Jr., J. Colloid Interface Sci., 61(3), 554 (1977).
48. Chiang, M.Y., Ph.D. Dissertation, University of Florida (1978).
49. Hsieh, W.C. and Shah, D.O., "The Effect of Chain Length of Oil and Alcohol as well as Surfactant to Alcohol Ratio on the Solubilization, Phase Behavior and Interfacial Tension of Oil/Brine/Surfactant/Alcohol Systems", SPE 6594, presented at the 1977 SPE-AIME Intl. Symposium on Oilfield and Geothermal Chemistry, LaJolla, CA, June 27-28, 1977.
50. Morgan, J.C., Schechter, R.S. and Wade, W.H., in "Improved Oil Recovery by Surfactant and Polymer Flooding", D.O. Shah and R.S. Schechter, eds., Acad. Press, Inc., N.Y. (1977).
51. Cash, R.L., Cayias, J.L., Fournier, G., Jacobson, J.K., Schares, T., Schechter, R.S. and Wade, W.H., "Modeling Crude Oils for Low Interfacial Tension", SPE 5813, presented at the SPE Symposium on Improved Oil Recovery, Tulsa, OK, March 22-24, 1979.
52. Satter, S.J., "The Influence of Type and Amount of Alcohol on Surfactant-Oil-Brine Phase Behavior and Properties," SPE 6843, presented at the 52nd Annual Fall Conference and Exhibition of SPE-AIME, Denver Co., Oct. 9-12, 1977.
53. Puerto, M.C. and Gale, W.W., "Estimation of Optimal Salinity and Solubilization Parameters for Alkyl Orthoxylene Sulfonate Mixtures", SPE 5814, presented at the SPE Improved Oil Recovery Symposium, Tulsa, OK March 22-24, 1976.
54. Vijayan, S., Ramachandran, C., Doshi, H. and D.O. Shah, in "Surface Phenomena in Enhanced Oil Recovery", D.O. Shah ed., pp. 327-376, Plenum Publishing Co., N.Y. (in press).

55. Bansal, V.K. and Shah, D.O., J. Colloid Interface Sci., 65(3), 451 (1978).
56. Bansal, V.K. and Shah, D.O., SPE J., 167 (June, 1978).
57. Bansal, V.K. and Shah, D.O., J. Am. Oil Chemists Soc., 55 (3), 367 (1978).
58. Vijayan, S., Ramachandran, C., and Shah, D.O., J. Am. Oil Chemists Soc., 58(4), 566 (1981).
59. Vijayan, S., Ramachandran, C. and Shah, D.O., J. Am. Oil Chemists Soc., 58(6), 746 (1981).
60. Vijayan, S., Ramachandran, C. and Doshi, H., "University of Florida Research on Chemical Oil Recovery Systems Semi-Annual Report", pp. B11-B57, June, 1978.
61. Cash, R.L., Cayias, J.L., Hayes, M., McAllister, D.J. Schares, T. and Wade, W.H., J. Pet. Tech., 985 (Sept. 1976).
62. Desai, N.N., in "University of Florida Research on Surfactant-Polymer Oil Recovery Systems-Annual Report", pp. I27-I49, Dec. 1979.
63. Desai, N.N., in "University of Florida Research on Surfactant-Polymer Oil Recovery Systems-Annual Report", pp. I35-I-48, Dec. 1980.
64. Hesselink, F. Th. and Faber, M.J., in "Surface Phenomena in Enhanced Oil Recovery," D.O. Shah, ed., pp. 861-869, Plenum Publishing Co., N.Y. (in press).
65. Chou, S.I. and Shah, D.O., in "Surface Phenomena in Enhanced Oil Recovery", D.O. Shah, ed., pp. 843-860, Plenum Publishing Co., N.Y. (in press)
66. Paul, G.W. and Froning, H.R., J. Pet. Tech., 25, 957 (1973).
67. Gupta, S.P. and Trushenski, S.P., SPE J., 19, 116 (1979).
68. Nelson, R.C., "The Salinity Requirement Diagram-A Useful Tool in Chemical Flooding Research Development", SPE 8824, presented at the SPE Improved Oil Recovery Symposium, Tulsa, OK, April 20-23, 1980.
69. Hirasaki, G.J., Van Damselaar, H.R. and Nelson, R.C., "Evaluation of the Salinity Gradient Concept in Surfactant Flooding", SPE 8825, presented at the SPE Improved Oil Recovery Symposium, Tulsa, OK, April 20-23, 1980.